THE STABILIZATION OF THE INITIAL PRODUCT OF THE PENTACYANIDONITROSYLFERRATE(II)-SULPHIDE REACTION AND ITS SPECTROPHOTOMETRIC APPLICATION

YIGA SOLOMON

BSc(Hons) (MAKERERE UNIVERSITY)

A DISSERTATION SUBMITTED TO THE GRADUATE SCHOOL IN PARTIAL FULFILLMENT OF THE REQUIREMENTS FOR THE AWARD OF THE DEGREE OF MASTER OF SCIENCE IN CHEMISTRY OF MAKERERE UNIVERSITY

NOVEMBER 2009

DECLARATION

I, Solomon Yiga solemnly declare that "**The Stabilization of the Initial Product of the Pentacyanidonitrosylferrate(II)-Sulphide Reaction and Its Spectrophotometric Application"** is my own piece of work, that it has never been presented to any Institution for any academic award, and that where other people's material has been used, due acknowledgement and appreciation has been extended.

…….

Solomon Yiga

This dissertation has been submitted for examination with the approval of the following Supervisors:

Professor Henry Ssekaalo

Dr. Jolocam Mbabazi

ACKNOWLEDGEMENT

I thank my supervisor, Professor Henry Ssekaalo, for the opportunity to study and work in his laboratory at the Chemistry Department, Makerere University. I am thankful for his support and guidance throughout my stay. I appreciate the many lively and fruitful discussions we had between us. I also want to thank my second supervisor, Dr. Jolocam Mbabazi, and the then Head Chemistry Department, Dr. Steven Nyanzi for their support and suggestions. I thank my lab mates, Adia Madina and especially Emmanuel Tebandeke, for their advice and technical assistance. I thank the International Programme in Chemical Sciences (IPICS) under SIDA Sarec Research grant for financial assistance.

I thank my parents, Mr. Israel Kamya and Mrs. Ruth Kamya for their moral support towards this study. Finally, I would like to express my deepest appreciation to my friends for their support throughout the course of completing this challenging educational endeavour.

TABLE OF CONTENTS

LIST OF TABLES

LIST OF FIGURES

LIST OF ABBREVIATIONS

ATP	Adenosinetriphosphate
DMPD	N,N-dimethyl-p-phenylenediamine
LoD	Limit of Detection
LoQ	Limit of Quantitation
NP	Nitroprusside
ppb	Parts per Billion
ppm	Parts per Million
RSD	Relative Standard Deviation
SD	Standard Deviation
SNP	Sodium Nitroprusside
UV-VIS	Ultraviolet-Visible

ABSTRACT

The effect of the cyanide ion on the reaction between the sulphide anion and excess nitroprusside both in the presence and absence of potassium chloride (KCl) as the ionic strength buffer is described. In the presence of KCl the cyanide ion stabilizes the initial product of the reaction, and directs its decomposition through a single pathway to the nitritopentacyanidoferrate(II). First order plots for the decomposition of the reaction product reveal an observed rate constant which varies linearly with the sulphide anion concentration.

In the absence of KCl, the cyanide ion dramatically stabilizes the red-violet initial product of the nitroprusside-suphide reaction, for a record period of up to 30 minutes and also enhances the absorbance of its solution.

A modified nitroprusside method for the determination of the sulphide ion in the presence of the cyanide ion by manual spectrophotometry is described. The limit of detection is 0.2 μg mL^{-1}, relative standard deviation of 2.4% for a 2.0 μg mL^{-1} sulphide ion and a working range of 0.3-5 μg mL^{-1} sulphide ion.

Other sulphur anions, such as the sulphite ion, that react with the nitroprusside in a similar way, do not interfere. The method was successfully applied to the determination of the sulphide anion in selected Uganda environmental systems: Kitagata hot springs water in south western part of the country, bathroom waste water, kitchen wastewater and boiled eggs.

CHAPTER ONE

INTRODUCTION

1.1 Background to the Study

Metal nitrosyls are complexes that contain transition metals bonded to nitrogen(II) oxide (NO). There are several bonding modes for the NO ligand, the most important being the terminal M-NO. A classic example in which this bonding mode is expressed is the pentacyanidonitrosylferrate(II) ion $[Fe(CN)_5NO]^{2-}$ commonly known as nitroprusside (NP), in which the NO is formally regarded binding as a 2-electron donor NO^+ [1]. In this complex the NO^+ ligand exhibits reactions with many nucleophiles like thiols, ketones, thioureas, sulphite anion, sulphide anion, compounds containing activated methylene groups, phenols, nitrils, uracils, pyrrols and indols, to form coloured products. The equation for the general reaction scheme is

$$[Fe(CN)_5NO]^{2-} + A^{n-} \longrightarrow [Fe(CN)_5NOA]^{(2+n)-} \qquad (1.1)$$

In most cases A^{n-} attacks the complex at the N atom , but attacks at O may also occur [2].

The reaction of interest in this work is that between NP and the sulphide anion (S^{2-}), which has been known for a long time to form a transient intense red-violet product [3]. It is of interest both from the theoretical and application points of view. Theoretically it demonstrates one of the few examples of ligand reactivity

in metal complex systems. Its well known application is the sensitive Gmelin test for the presence of S^{2-}.

Despite the above outlined importance of this reaction, only scarce literature exists on its kinetic and mechanistic parameters [4]. The analytical uses of this reaction also appear scarce [5, 6] and are not well developed. As a result, the reaction has not been of wide application in the quantification of S^{2-}.

1.2 Problem Statement

The reddish-violet product formed in the NP-S^{2-} reaction is transient. This has made its application in the spectrophotometric determination of the sulphide anion using manual instrumentation unsuccessful. Yet from the cost point of view, this is the technique of choice if it were not for this limitation. Therefore, stabilization of the reaction product is of utmost importance in the application of this reaction for the determination of the S^{2-} using manually operated spectrophotometers.

1.3 Objectives of the Study

The overall objective of the study was to stabilize the initial product of the NP-S^{2-} reaction and develop a method basing on the stabilized product of this reaction for the determination of micro quantities of S^{2-} in environmental systems. This was to be achieved by the following specific objectives:

(a) To introduce stabilizers known for other NP reactions into the NP-S^{2-} reaction and study the kinetics of decomposition of the product.

(b) To develop and validate a manual spectrophotometric method for the quantification of micro quantities of S^{2-} based on the modified reaction conditions.

(c) To apply the developed and validated method for S^{2-} determination in selected environmental systems.

1.4 Justification of the Study

The current standard method recommended for S^{2-} analysis is the methylene blue method based on the oxidative coupling of two molecules of N,N-dimethyl-p-phenylenediamine (DMPD) with S^{2-} to form a thiaazaheterocyclic dye [7]. The method is very expensive and involves aggressive reagents [5].

Other affordable methods that include volumetric analysis have been approved by the United States Environmental Protection Agency [8]. The methods however suffer from a number of interferences from reducing species. The spectrophotometric nitroprusside method seems to be an attractive alternative for the determination of S^{2-} especially in microquantities. Its use has been restricted to automated procedures using auto analyzers where the colour is measured after a definite time from addition of the reagents [9, 10]. However, automated instrumentation systems are not available in many analytical and research laboratories. Stabilizing the initial reaction product will enable a manual procedure for determining the anion, which is within the means of most laboratories.

1.5 Literature Review

1.5.1 Bonding behaviour of nitrogen(II) oxide in nitrosyl complexes

The NO which is a ligand in metal nitrosyl complexes has the electron configuration $\sigma 1s^2, \sigma^* 1s^2, \sigma 2s^2, \sigma^* 2s^2, \sigma 2p_x^2, \pi 2p_y^2, \pi 2p_z^2, \pi^* 2p_y^1, \pi^* 2p_z^0, \sigma^* 2p_x^0$ whose molecular orbital energy diagram is shown in Figure 1 [11].

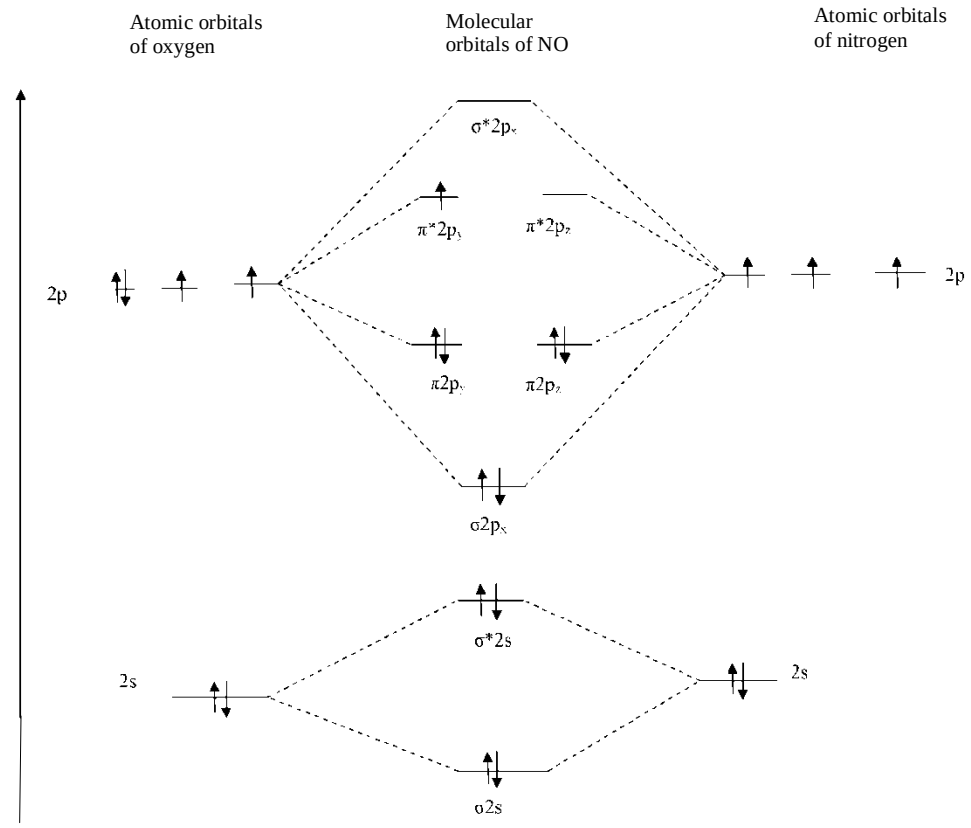

Figure 1: Molecular orbital energy diagram of nitrogen(II) oxide.

Just as the carbon monoxide (CO) group reacts with a metal atom that presents an empty σ orbital and a pair of filled dπ orbitals to give a linear MCO grouping with a C→M σ bond and a significant degree of M→C π bonding, so does the NO group which engages in a structurally and electronically analogous reaction with a

metal atom. The metal centre may be considered, at least formally, to present an empty σ orbital and a pair of dπ orbitals containing only three electrons. The full set of four electrons for the Mdπ→ π*(NO) interactions is thus made up of three electrons from M and one from NO [11]. In effect NO contributes three electrons to the total bonding configuration, the two electrons being for the sp orbital on the N atom in formation of the N→M σ bond .

This bonding mode is applicable when the M-N-O group is close to 180^{o} (linear nitrosyl) and bonds as NO^{+} which is isoelectronic to CO. Such charge transfer from the σ*NO orbital to the metal is qualitatively consistent with the relatively high ν_{NO} stretching frequencies shown in Table 1 (~1,800-1,950 cm^{-1}) usually observed for these species and reflects the triple-bond character of the N-O bond [12]. The bent MNO coordination implies less electronic charge transfer from NO to M, and consequently the ν_{NO} values are lower. As the angle approaches 120°, the polarity of the charge transfer is reversed and the ligand is formally a nitroxyl anion (NO^{-}) [12].

Table 1: Some examples of linear and bent coordination of nitrogen(II) oxide

Example	**M-N-O angle**	**ν (N-O)/cm^{-1}**
$Na_2[Fe(CN)_5(NO)].2H_2O$	178^{0}	1935
$Na_2[Ru(NO)(NO_2)(OH)].2H_2O$	180^{0}	1893
$[CoCl(en)_2(NO)]ClO_4$	124^{0}	1611
$[Ir(CH_3)I(NO)(PPh_3)_2]$	120^{0}	1525

In view of the differences between the electronic structures of linear and bent bonding modes, considerable differences in their chemical reactivity are expected. In general, linear MNO groups are attacked by nucleophiles while bent ones, due to a lone pair on N are susceptible to electrophilic attack, but this is by no means a rule and there are many exceptions [2].

1.5.2 Electrophilic reactions of nitrogen(II) oxide ligand in nitrosyl complexes

The electrophilic behaviour of the NO ligand is illustrated by the long known reversible reaction of the hydroxide anion with the NP ion shown in Equation 1.2.

$$[Fe(CN)_5NO]^{2-} + 2OH^- \longrightarrow [Fe(CN)_5NO_2]^{4-} + H_2O \qquad (1.2)$$

The rate of this reaction is first order in $[OH^-]$ and in $[Fe(CN)_5NO^{2-}]$ [13], so the likely reactive intermediate is the adduct $[Fe(CN)_5(NO)(OH)]^{3-}$. The reaction is reversed in strongly acidic solution. Similar reactions are observed with the ruthenium [14] and osmium analogues [15]. The reaction of $Os(CN)_5(NO)^{2-}$ with the hydrosulphide ion (SH^-) leads to the loss of the NO^+ and formation of $Os(CN)_5(H_2O)^{3-}$, which can be trapped by the addition of pyrazine [15]. Notably, the reactions of the $M(CN)_5(NO)^{2-}$ anions with the SH^- anion are much faster than the analogous reactions with OH^-; the rate constants k_{SH} (M) are several orders of magnitude larger than the k_{OH} (M) values for the same complexes [15].

In general the interaction of the nitrosyl complex with the nucleophiles forms a 1:1 adduct, with the nucleophiles bound to the N atom. The general mechanistic procedure comprises an initial equilibrium between the nitrosyl-complex and the

nucleophiles with the ensuing decomposition of the adducts, leading to the reduction of NO^+ and the oxidation of the nucleophiles [16]. For the above reaction to be favoured the N atom centre must possess a net positive charge as $\overset{+}{N}O$ by donation of its unpaired π antibonding electron to the metal. The adduct formation rates increase with more positive charge at the electrophilic N atom [16]. The typical intense colour of the adduct fades in all studied complexes. This is attributed to the weak N-nucleophile bond which undergoes a facile breakage.

1.5.3 The nitroprusside anion

The NP anion ($[Fe(CN)_5NO]^{2-}$) was first prepared by Lyon Playfair as a sodium salt [17]. Most of the preparative reactions described to make NP are between sodium hexacyanoferrate(II) or (III) and nitric acid or sodium nitrite [18] summarized by the following respective equations:

$$[Fe(CN)_6]^{4-} \xrightarrow{HNO_3} [Fe(CN)_5NO]^{2-} \qquad (1.3)$$

$$2Na_4Fe(CN)_6 + 2NaNO_2 + 3BaCl_2 + 3CO_2 + H_2O \longrightarrow 2Na_2Fe(CN)_5NO + 2HCN + 3BaCO_3 + 6NaCl \qquad (1.4)$$

1.5.3.1 Structure of the nitroprusside anion

The crystal structure of sodium nitroprusside (SNP) was determined in 1963 by X-ray diffraction techniques [19]. The anionic complex has an octahedral structure as shown in Figure 2. On the basis of spectroscopic and magnetic evidence [2], the bonding mode for NO in this complex is linear M-NO. The NO is formally regarded binding as a 2e donor NO^+ having transferred its odd

electron to Fe^{3+} thus lowering the formal oxidation state of the metal. NP is a $\{FeNO\}^6$ species and its description as $Fe^{II}NO^+$ is generally accepted [2].

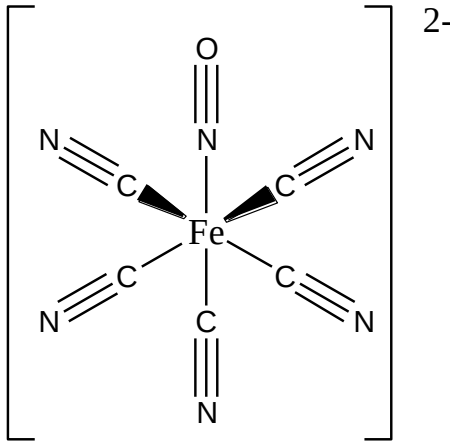

Figure 2: Structure of the pentacyanidonitrosylferrate(II) anion.

Nitrosyl transition metal complexes are in general extensively studied because of their long-lived metastable states which are easily obtained by irradiation with light. In the case of SNP, two light-induced metastable states have been observed using Mössbauer spectroscopy [20]. They are produced by blue light irradiation and annihilated by red light irradiation. In crystaline SNP, metastable states have lifetimes greater than 104 s at temperatures below 140 K. Because of this property, nitrosyl transition metal complexes attracted the interest of many researchers as potential candidates for functional material of memory devices [21-23] in which information can be optically written, read and erased.

The structures of the two metastable states of SNP and that of its ground state have been analysed by X-ray diffraction at 50 K [24]. Structural changes are

mainly confined to the Fe-N-O group. In this respect, the ground state is linear, of symmetry C_{4v}, with the iron bound to the nitrogen atom as shown in Figure 2.

Figure 3 shows the structure of the two metastable states in which one is also linear, but with the iron bound to the oxygen atom (isonitrosyl, η^1). In literature, this metastable state is often labeled MS_I and its presence has been further confirmed by nuclear light scattering studies [25]. The second metastable state, which has C_s symmetry (Figure 3), has the NO bound sideways (η^2). This metastable state is usually labeled as MS_{II}.

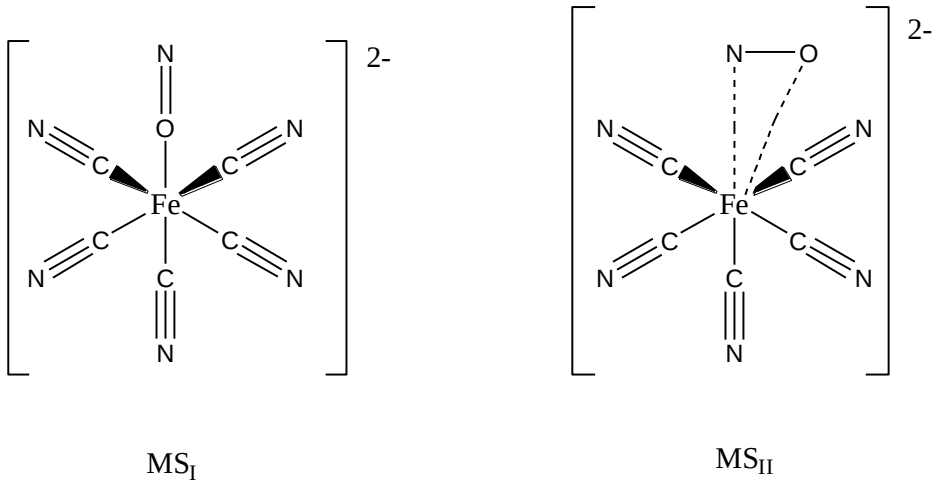

MS_I MS_{II}

Figure 3: Proposed structures of the metastable states of the nitroprusside anion.

1.5.3.2 Reactions of the nitroprusside anion

NP undergoes a number of reactions with many nucleophiles. Some of its reactions are illustrated below.

It reacts with mercaptans (RSH) and mercaptides (RS^-) to form metal nitrosothiolato intermediates with deep red or purple colours [26]. These

intermediates are unstable and decay via formation of disulfides and reduced nitroprusside, which subsequently decomposes by both cyanide and NO loss.

In pH 10.5 solutions with relatively high ammonia concentrations, NH_3 reacts with nitroprusside to give $Fe(CN)_5(H_2O)^{3-}$ plus N_2. This reaction is effectively the comproportionation of NH_3 and NO^+ to N_2 [27, 28].

Likewise, primary amines RNH_2 are diazotized by aqueous NP to give the alcohols plus N_2, with the maximum rate occurring about pH 10.5 [29]. The rates of these reactions are first order in [NP] and [RNH_2] and increase with the basicity of the amines. The protonated amines are not reactive. At higher pH, nitroprusside reacts with OH^- to give $[Fe(CN)_5(NO_2)]^{4-}$ [29].

1.5.3.3 Uses of the nitroprusside anion

NP has been put to several useful applications. Its sodium salt (SNP) under the pharmacological and commercial name nipride is an effective vasodilator in lowering blood pressure. It is widely used to induce hypotension during surgery [30]. It has also been used, in a similar manner, in the treatment of chronic hypertension and in the management of myocardial infarction and other cardiac failure conditions [31]. Nipride can produce nitrogen(II) oxide which activates guanylate cyclase. Guanylate cyclase results in increased concentrations of cyclic guanosine monophosphate in smooth muscle, leading to vasodilation of veins and arteries [32]. In summary nipride is an effective drug for the treatment of two conditions, high blood pressure and heart attack, which are common and wide-spread.

For over a century SNP has also been used as an analytical reagent for the qualitative and quantitative analysis of organic and inorganic compounds illustrated by the following examples. It is used as an indicator in the volumetric determination of halides, cyanides and the estimation of mercuric acetate in non-aqueous solvents [33]. Its use as an indicator is proposed in the mercumetric estimation of chloride formed on the hydrolysis of chlorobutanol, and it is used in conjunction with certain dyes as an indicator in the estimation of reducing sugars [33].

The intense yellow colour given by SNP and caustic alkalis or alkaline-earth hydroxides serves to indicate the presence of these compounds. In general the use of SNP for the qualitative and quantitative analysis of cations is based on the formation of insoluble nitroprussides.

All sulphur bearing anions give colorations with SNP. For example SNP has been used in the determination of the sulphite anion where it forms a red complex whose colour is intensified in the presence of alkali metal ions [34].

SNP has also been thoroughly investigated as a reagent for carbonyls and compounds which may be converted to them [33]. It is also used in the analysis of hydrocarbons, phenols, amino derivatives, sulphur compounds, heterocyclics, and other organic compounds [33]. Further, it is used to detect and estimate hydrosulphide derivatives, amino acids, polypeptides and proteins containing sulphur. It is also used for microbiological tests, blood and urine analysis [35].

1.5.4 The suiphide anion

The S^{2-} anion is a major species of sulphur in which the -II state is expressed. It is often present in ground water, especially in hot springs due to geochemical processes in hydrothermal systems [7]. Its common presence in wastewaters comes partly from industrial wastes, petroleum and petrochemical plants, gas works, paper mills, heavy water plants and tanneries, but mostly from anaerobic bacterial reduction of the sulphate, or sulphur-containing compounds [7].

The dissolved S^{2-} can react with the hydrogen ions in water to form the HS^- anion or hydrogen sulphide (H_2S) gas. The relative concentrations of these species are a function of the pH of the water; H_2S concentrations increase with decreasing pH [36]. In polluted waters, therefore, where the pH can be neutral or acidic, the potential for H_2S formation is increased.

1.5.4.1 Biological effects of hydrogen sulphide

H_2S is a colourless, flammable, water soluble gas with a characteristic odour of rotten eggs which can be smelled by some people even at a very low concentration of 0.5 ppb in air [37]. H_2S exerts a host of biological effects on various biological targets resulting in responses that range from toxic effects to protective actions.

Toxic effects of inhaled H_2S at relatively high acute exposure levels or at chronic lower-level exposure include olfactory epithelial toxicity and a transient loss of olfaction. The chief toxic effects are associated with the deactivation of enzymes, either through the cleavage of their disulphide bridges or by the coordination of

S^{2-} to metal co-factors such as Fe^{2+}, Mg^{2+} or Cu^{2+}. In this manner, key enzymes such as cytochrome oxidase, alkaline phosphatase and carbonic anhydrase can be irreversibly denatured. The human body detoxifies H_2S by oxidizing it into sulfate or thiosulfate by hemoglobin-bound oxygen in the blood or by liver enzymes [33]. Lethal toxicity occurs when H_2S is present in concentrations high enough to overwhelm the body's detoxification capacity [33].

At micromolar concentrations, multiple studies have demonstrated the protective/ therapeutic effects of H_2S as illustrated in the following examples.

H_2S has the ability to neutralize a variety of reactive species in the body including oxyradicals [38] , peroxynitrite [39], hypochlorous acid [40] and homocystein [41] . It is also known to induce an upregulation of anti-inflamatory and cytoprotective genes including haemoxygenase in pulmonary smooth muscle cells [42]. H_2S is related to the opening of potassium-opened adenosine triphosphate channels [43] which regulate pancreatic insulin regulation.

H_2S has been used to put mice into a state of reversible metabolic hibernation dramatically reducing their core body temperature, respiration and need for oxygen [44]. This envisions a future in which similar techniques could be used to "buy time" for critically ill patients who otherwise would face injury and death from insufficient blood and oxygen supply to organs and tissues [44].

H_2S has also been shown to significantly increase life span and heat tolerance in the nematode worm *Caenorhabditis elegans* whose biology is similar in many

respects to that of humans [45]. Understanding how H_2S affects the physiology in animals may lead to the development of drugs that could delay the onset of age-related diseases in humans such as cancer, Alzheimer's and heart disease [45].

Because the therapeutic potential of H_2S is an entire field, the reader is referred to detailed expert reviews on this subject [46]. This potential probably justifies the reason as to why most H_2S-containing hot-spring water is linked to the curative treatment of ailments.

Hence, the determination of S^{2-} is of utmost importance in the control and monitoring of both toxic and therapeutic H_2S emissions, especially from wastewater and natural water.

1.5.4.2 Determination of the sulphide anion

A number of techniques have been developed to quantify total sulphide species (H_2S + HS^- + S^{2-} + reactive polysulphides). These include spectrophotometric methods with methylene blue [7], ethylene blue [47], nitroprusside [5, 6], copper quin-8-olate [48] and direct measurement [36]. A variety of other methods using spectrofluorimetry, flow injection analysis, gas chromatography and polarography have been used to quantify S^{2-} as well [49].

Spectrophotometric methods are easier to use and a review of existing literature indicates that the methylene blue [7] method is the basis of current standard manual methods.

A spectrophotometric method worth special consideration is based on the formation of a transient red-violet product from the nitroprusside-sulphide reaction. The reaction for this method has been known even longer but it is disadvantaged by the transience of the coloured product. However the method has been proposed to be of satisfactory use in automated systems. A literature search shows that little has been done concerning the chemistry of the reaction of this method in terms of the identity of the reaction product and its decomposition pathways. A review of these aspects is undertaken below.

1.5.5 The nitroprusside-sulphide reaction

The origin of the nitroprusside-sulphide ($NP\text{-}S^{2-}$) reaction is traced back from Gmelin's first observation of the colour reaction between sulphides and the reaction product from nitric acid and potassium ferricyanide [33]. This observation was made a year before nitroprussides were first synthesized, and from that time up to present day the $NP\text{-}S^{2-}$ colour reaction is called Gmelin's reaction [33]. NP reacts with S^{2-} to form a transient reddish-violet coloration which is intense to detect a concentration of 0.02 mg of Na_2S per cm^3 [3]. Electrometric studies showed that a large drop in E.M.F occurs when one mole of NP has been added to one mole of Na_2S [3], according to the equation

$$[Fe(CN)_5NO]^{2-} + S^{2-} \longrightarrow [Fe(CN)_5NOS]^{4-} \qquad (1.5)$$

The reaction product is however unstable and fades to finally form clear solutions reported to contain ferrooxide and ferrocyanide [3]. The kinetics of the fading

product in excess S^{2-} has also been determined and the reaction was observed to have a half-life of 81 seconds at 293 K [4].

There exists doubt on the nature of the product of this reaction. It has been reported by various workers as $[Fe(CN)_5NOSH]^{3-}$ [4], $([Fe(CN)NOS_2]^{6-}$ [6]. A recent review of the reaction and its analytical use [5], proposes $[Fe(CN)_5NOS]^{4-}$ as the initial product (λ_{max}538 nm) which then undergoes a redox reaction to form oligomeric/polymeric structures (λ_{max}572 nm).

1.5.6 Development and validation of the nitroprusside-sulphide method for sulphide anion determination

Method development is the setting up of an analytical procedure that will be appropriate for the analyte of interest. This may involve adopting an existing method by optimizing the reaction conditions of the procedure, or use a new reaction for the same analyte [50].

The development of the NP-S^{2-} method for sulphide anion determination involves among others the stabilization of the unstable coloured product. In an attempt to stabilize the coloured reaction product, a strongly alkaline reaction medium has been proposed by a number of workers [5, 6]. However, this can only stabilize the product for as short as 150 seconds for low S^{2-} concentrations and a much shorter period at high concentrations [5].

A number of stabilizing agents have been used on the reactions of NP with other nucleophiles. These include alkali metal cations and zinc which have been used as intensifying and stabilizing agents in the NP-sulphite reaction [34]. The cyanide

ion (CN^-) [51] and hydroxyquinoline [52] have been reported to reduce the fading of the coloured reaction product of the NP-glutathione reaction. In addition CN^- has also been reported to stabilize the coloured reaction product of the NP-cysteine reaction [53].

Method validation can be defined as the process of establishing the performance characteristics and limitations of a method and the identification of the influences which may change these characteristics and to what extent. It also includes which analytes the method can determine, in which matrices and in the presence of which interferences. Within these conditions validation also determines what levels of precision and accuracy that can be achieved.

To be fit for the intended purpose, the method must meet certain validation characteristics. Typical validation characteristics, which should be considered, are: method detection levels, selectivity, linearity, range, accuracy, precision, limit of detection and quantitation [50].

This work aims at a further stabilization of the initial product of the NP-S^{2-} reaction, validation of the modified method and eventually use of the reaction for S^{2-} determination using manual spectrophotometry.

CHAPTER TWO

EXPERIMENTAL

2.1 Apparatus

Weighing was done on an AAA 160DL dual range balance (Adam Equipment Co. Ltd UK). The absorption spectra were recorded on a UV-VIS Shimadzu UV-1700 CE double beam spectrophotometer (Shimadzu Corporation Japan) and absorbance measurements at a fixed wavelength were made with the same instrument in the photometric mode. pH measurements were done with a Corning Pinnacle 555 pH/ion meter (Corning Incorporated Life Sciences Corning, New York 14831 USA). The addition of aqueous NP to aqueous S^{2-} was carried out using Transferpette micropipettes (BRAND GMBH + CO KG Postfach 11 55 97877 Wertheim Germany).

2.2 Materials

All chemicals used were of reagent grade. They included: potassium chloride, potassium cyanide, sodium hydroxide, sodium nitroprusside dihydrate, disodium hydrogen phosphate, potassium iodide, iodine, sodium thiosulphate pentahydrate, zinc acetate, potassium bi-iodate and sulphuric acid. Deionized water was used for preparation of all aqueous solutions.

2.2.1 Starch indicator solution

The starch indicator solution was prepared by dissolving laboratory grade soluble starch (2 g) and salicylic acid (0.2 g) in hot deionized water (100 mL).

2.2.2 Standard potassium iodate solution

A 0.0021 M potassium iodate solution was prepared by dissolving $KH(IO_3)_2$ (812.4 mg) in deionized water and diluted to 1000 mL.

2.2.3 Standard sodium thiosulphate

$NaS_2O_3.5H_2O$ (6.204 g) was placed in a volumetric flask (1000 mL) and dissolved in deionized water (50 mL). NaOH (0.4 g) was added and the solution brought to the mark with deionized water. The solution was then standardized using a standard $KH(IO_3)_2$ solution as follows. KI (2 g) was dissolved in an Erlenmeyer flask with deionized water (150 mL). Concentrated H_2SO_4 (3 drops) and standard $KH(IO_3)_2$ solution (0.0021 M, 20 mL) were added respectively. The solution was diluted to 200 mL and the liberated I_2 titrated against NaS_2O_3 titrant with starch as the indicator. The concentration of sodium thiosulphate was found to be 0.025 M.

2.2.4 Standard iodine solution

KI (25 g) was dissolved in a little water and I_2 (3.2 g) added. After I_2 had dissolved, it was diluted to 1000 mL and standardized against NaS_2O_3 (0.025 M) using starch solution as indicator. The standardized iodine solution was 0.0125 M

2.2.5 Sodium sulphide stock solution

Fresh S^{2-} stock solutions were prepared by bubbling H_2S in a 10% NaOH solution as shown in Figure 4. H_2S was prepared by reacting FeS with dilute HCl. Determination of S^{2-} was carried out iodimetrically. Intermediate standard S^{2-} solutions were prepared by dilution of the stock solutions with 25 mM NaOH.

2.2.6 Aqueous sodium nitroprusside

Fresh stock aqueous SNP (0.02 M) was used. This was prepared by dissolving SNP crystals (6 g) in deionized water and the volume made up to 1000 mL.

2.2.7 Buffer solution

For the pH range of 11.0-11.5 a phosphate buffer was used. This was prepared by mixing aqueous Na_2HPO_4 (100 mL, 0.05 M) and aqueous NaOH (20 mL, 0.1 M).

2.2.8 Aqueous zinc acetate solution

Zinc acetate (220 g) was dissolved in deionized water (870 mL). The solution was made up to one litre.

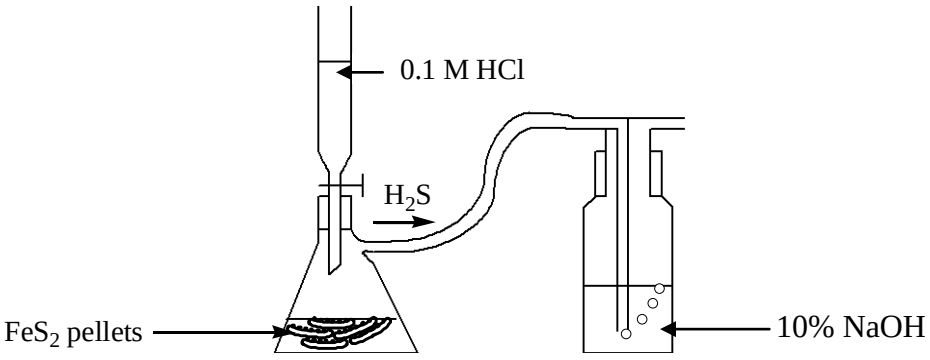

Figure 4: Schematic diagram for the apparatus used to prepare sodium sulphide stock solution.

2.3 Iodimetric Determination of the Sulphide Anion

Before determining the S^{2-} concentration in a sample, interferences due to SO_3^{2-}, $S_2O_3^{2-}$, and other soluble reductants had to be eliminated by precipitating the S^{2-} as ZnS, followed by removing the supernatant solution and replacing it with

deionized water. This was done by putting aqueous zinc acetate (0.2 mL) into a glass bottle (100 mL) which was then filled with the sample and NaOH (0.1 mL, 6 M) added. The mixture was then shaken vigorously. The precipitate was collected on cellulose free filter paper and titrated immediately with I_2 as follows.

Standard I_2 (0.0125 M) was measured from a burette into a 500 mL conical flask. Deionized water was added to bring the volume to 20 mL. HCl (2 mL, 6 M) was then added. The ZnS precipitate plus filter papers were introduced under the solution surface and the solution was then stirred. The excess I_2 was back titrated against standard NaS_2O_3 (0.025 M) using starch as the indicator.

2.4 Reaction of Nitroprusside with Sulphide Anion in the Presence of Stabilizing Species

To an aliquot of intermediate standard aqueous S^{2-} (50-200 µL) in a volumetric flask (10.0 mL) was added; phosphate buffer (1 mL) to adjust the pH within a range of 11-12, aqueous stabilizer of known amount and aqueous NP (100 µL, 0.02 M). The mixture was diluted to the mark by addition of an appropriate amount of deionized water and uniformly mixed for five seconds. The resultant red-violet solution was immediately transferred to cuvettes which were inserted in the spectrophotometer for scanning its spectrum.

2.4.1 Spectral characterization of the reaction mixture

The absorption spectrum of the solution was obtained by carrying out a spectral run in the UV-VIS region. Time-dependent spectra of the reaction mixture were obtained from successive spectral runs after intervals of 25 seconds.

2.4.2 Kinetic studies

Kinetic measurements were performed spectrophotometrically, as described below, with at least a 10-fold excess of NP over the S^{2-} concentration, at pH 11, using known concentration of the stabilizer. Micro pipette syringes were used to take the required volumes of each solution, and deliver them in a volumetric flask (10 mL) where mixing was done and made up to the mark. The resultant solution was put in a 1 cm quartz tandem cell and placed in the spectrophotometer for characterization. The effect of an introduced stabilizer on the reaction product was studied at 25.5 ± 0.1 ^{o}C for a S^{2-} concentration in the range 0.035 to 0.1 mM and NP concentration in the range 0.23 to 1.8 mM. The observed rate constant, k_{obs} (s^{-1}), was obtained by fitting the kinetic traces at 534 nm to a single exponential function by means of a Microsoft Excel Solver. All measurements were repeated three times and reported values are the average of the three measurements. The error was estimated from the standard deviation of these measurements.

2.4.3 Spectrophotometric determination of the sulphide anion

The determination of the sulphide anion concentration in a sample after reacting it with NP in the presence of a known stabilizer was done by reading off the stable absorbance reading at λ_{max} 534 nm and then using a pre-prepared absorbance vs concentration calibration curve to determine the concentration. This concentration was then compared to the one obtained by iodimetry.

2.5 Method Development and Validation

A validation was carried out on the developed method and the following characteristics determined: method detection limits, selectivity, linearity, range, accuracy, precision and recovery. Each one of these is described below.

2.5.1 Determining detection and quantification limits

The limit of detection (LoD) is the lowest concentration of analyte in a sample that can be detected but not necessarily quantifiable under stated conditions of the test. The LoD in this work was determined by analyzing 10 independent sample blanks whose standard deviation (SD) was calculated. LoD was then expressed as the analyte concentration corresponding to the mean sample blank value + 3SD [50]

The limit of quantification (LoQ) is the lowest concentration of analyte that can be determined with an acceptable level of repeatability, precision and trueness. The LoQ in this work was determined by analyzing 10 independent sample blanks whose SD was calculated. LoQ is expressed as the analyte concentration corresponding to the mean sample blank value + 10SD [50].

2.5.2 Selectivity

The interference due to several cationic and anionic species was studied. Different amounts of ionic species were added to a S^{2-} solution of known concentration. The extent of interference caused by each species was then studied.

2.5.3 Working range and linearity

Working range refers to the range of concentrations over which the method may be applied whereas linearity refers to the ability of the method to obtain test results proportional to the concentration of the analytes [50]. A plot of measurement response against measurand concentration was made. A visual examination to identify approximate linear range, upper and lower boundaries of the working range was done. LoQ forms the lower end of the working range. The linearity was obtained from the correlation coefficient value (R^2) of the line of best fit (least-squares line).

2.5.4 Accuracy and precision

Accuracy is defined as nearness to the true value [50]. It was determined by calculating the mean recovery of the spiked seven portions of standard S^{2-} solutions at slightly above and lower than the detection level. It is defined by the relation

$$\text{Accuracy} = \frac{y}{z} \times 100\% \qquad (2.1)$$

where y = mean value of seven replicates

z = spiked concentration

Precision is a measure of how close results are to one another, and is usually expressed by measures such as SD and percent relative standard deviation (RSD), which describe the spread of results. Precision was determined by calculating both

SD and RSD of the spiked analyte recoveries for seven replicates at different concentrations and defined by the relations of Equations 2.2 and 2.3 respectively.

$$\mathrm{SD} = \sqrt{\frac{1}{\mathrm{n}-1}\sum_{i=1}^{n}(x_i - \bar{x})^2} \tag{2.2}$$

where $\bar{x}$ = mean value of the seven replicates

n = number of samples analyzed

$$\mathrm{RSD} = \frac{\mathrm{SD}}{\mathrm{y}} \times 100\% \tag{2.3}$$

where SD = standard deviation for seven replicates

y = mean value of seven replicates.

From SD, the repeatability limit (*r*) which enables the analyst to decide whether the difference between duplicate analyses of a sample determined under repeatability conditions is significant was calculated based on the relation

$$r = t_{\infty} \times \sqrt{2} \times \mathrm{SD} \tag{2.4}$$

where t_{∞} is the Student's two tailed value for v = ∞ for a given confidence (normal confidence level state is 95% where the value is 1.96), and SD is the standard deviation measured under repeatability conditions [50].

2.6 Determination of the Sulphide Anion in Selected Environmental Systems

2.6.1 Environmental systems investigated

The method of the NP-S^{2-} reaction based on conditions of the present work was applied to the determination of S^{2-} in water from five environmental systems in Uganda as described below:

- Hot spring water from Kitagata (0^o 40' 00.24" S, 30^o 09' 00. 24" E) located in Bushenyi district found in the south-western part of Uganda. The water was collected from two close hot springs of Kitagata: Kitagata hot spring 1 usually called royal spring is free from human disturbance; Kitagata hot spring 2 which is disturbed by people who bathe in the water.
- Bathroom wastewater kept in anaerobic conditions. This wastewater was personally generated by taking a bath using commercially available bathing soap that contains a sulphur-based detergent and surfactant called sodium lauryl ether sulfate ($CH_3(CH_2)_{10}CH_2(OCH_2CH_2)_{13}OSO_3Na$). The wastewater was collected and kept in a basin which was covered to simulate anaerobic conditions present in pits which collect bathroom wastewater. After a period of 24 hours, the water was filtered and analysed for S^{2-}.
- Seven boiled eggs were collected from a local canteen from Makerere University. Shells were removed, and each egg was crashed and placed in a 250 mL cornical flask containing sulphuric acid (0.01 M, 100 mL). The mixture was heated to 40 ^oC for 30 minutes and the distillate was collected

in a solution of sodium hydroxide (25 mL, 0.025 M) and analysed for S^{2-} anion content.

- Water samples were also collected from foul smelling stagnant wastewater of a blocked drainage manhole (Figure 5). This was wastewater from the kitchen of Michelle Hall of residence at Makerere University.

Figure 5: Stagnant kitchen wastewater of a blocked drainage manhole at Mitchelle Hall of residence, Makerere University.

2.6.2 Sample preparation

The samples were made alkaline by adding sodium hydroxide pellets (0.2 g per 1000 mLs of sample) and then tightly covered. This was done to avoid loss of S^{2-} as H_2S which occurs in acidic conditions.

The pH of the samples was buffered to pH 11.5 (phosphate buffer). This was done by adding Na_2HPO_4 (1.42 g) and NaOH (0.2 g) to the sample (100 mL). The samples were filtered to remove any solid particles that were present. A known amount of stabilizer was added to the filtrate which was then ready for analysis.

CHAPTER THREE

RESULTS AND DISCUSSION

3.1 Stabilization of the Initial Product of the NP-S^{2-} Reaction

In reference to the technique of employing alkali metal cations as stabilizing agents for the NP-sulphite reaction [34], potassium and sodium cations were introduced separately into aqueous S^{2-} as chloride salts. Upon addition of excess aqueous NP (9-fold) to aqueous S^{2-} containing alkali cations (potassium or sodium) as stabilizers, the solutions immediately became purple and faded to yield a yellow solution. The UV-VIS absorption spectrum showed two different products formed with maximum absorption peaks (λ_{max}) at 534 nm and 398 nm. The peak with λ_{max} 534 nm is attributed to the red-violet initial reaction product of the NP-S^{2-} reaction and λ_{max} 398 nm is attributed to the yellow final product.

The introduction of the alkali cations caused a significant increase in the absorbance due to the initial reaction product compared to when the alkali cations were absent. However, no specific cationic effect was observed. Figure 6 shows a representative spectrum obtained from a solution containing 1 M KCl compared to that when it was absent. Time-dependent spectra of the solution are also shown in Figure 7.

For the intended purpose of stabilizing the initial product to be fit for the determination of microquantities of S^{2-}, the stability of the coloured complex was studied by running spectral scans for the reaction at specified time intervals up to

twenty four minutes. Figure 8 shows the time-dependent spectra obtained for the stability studies in the presence of KCl. The spectral characteristics of the reaction indicate that the initial reaction product still has a high degree of instability in the presence of chlorides of alkali metals. Other alkali salts other than the chlorides were also tested to determine the effect of anions on the stability of the initial reaction product. These included: sulphates, bromides, nitrates and cyanides. With the exception of the cyanides, all the other anions had intensification and stabilizing effects on the initial reaction product similar to those obtained with the chlorides. The cyanides however showed a remarkable intensification of the colour and stabilization of the initial reaction product.

The effect of cyanide was studied at ionic strength of 1 M KCl by including KCN in the reaction mixture. Figure 9 shows that the presence of cyanide caused a further increase in the absorbance of the initial reaction product. The rate of decomposition of the initial product was also reduced as shown by time-dependent spectra of this product in Figure 10, which also shows a distinct isosbestic point at 465 nm that was not shown by other anions tested in this work.

A stability study was carried out in the presence of CN^- and in its absence as shown in Figure 11. The figure shows a dramatic persistence of the initial reaction product in the presence of CN^- even after a period of thirty minutes. This persistence of the peak after a period of thirty minutes shows a novel and dramatic stabilizing effect of the initial product that the CN^- introduces in this reaction. In addition to the stabilizing effect of CN^-, Figure 11 also shows that in the presence

of CN^-, the product with λ_{max} 325 nm decomposes to other products which were not optically identifiable using UV-VIS spectrophotometry.

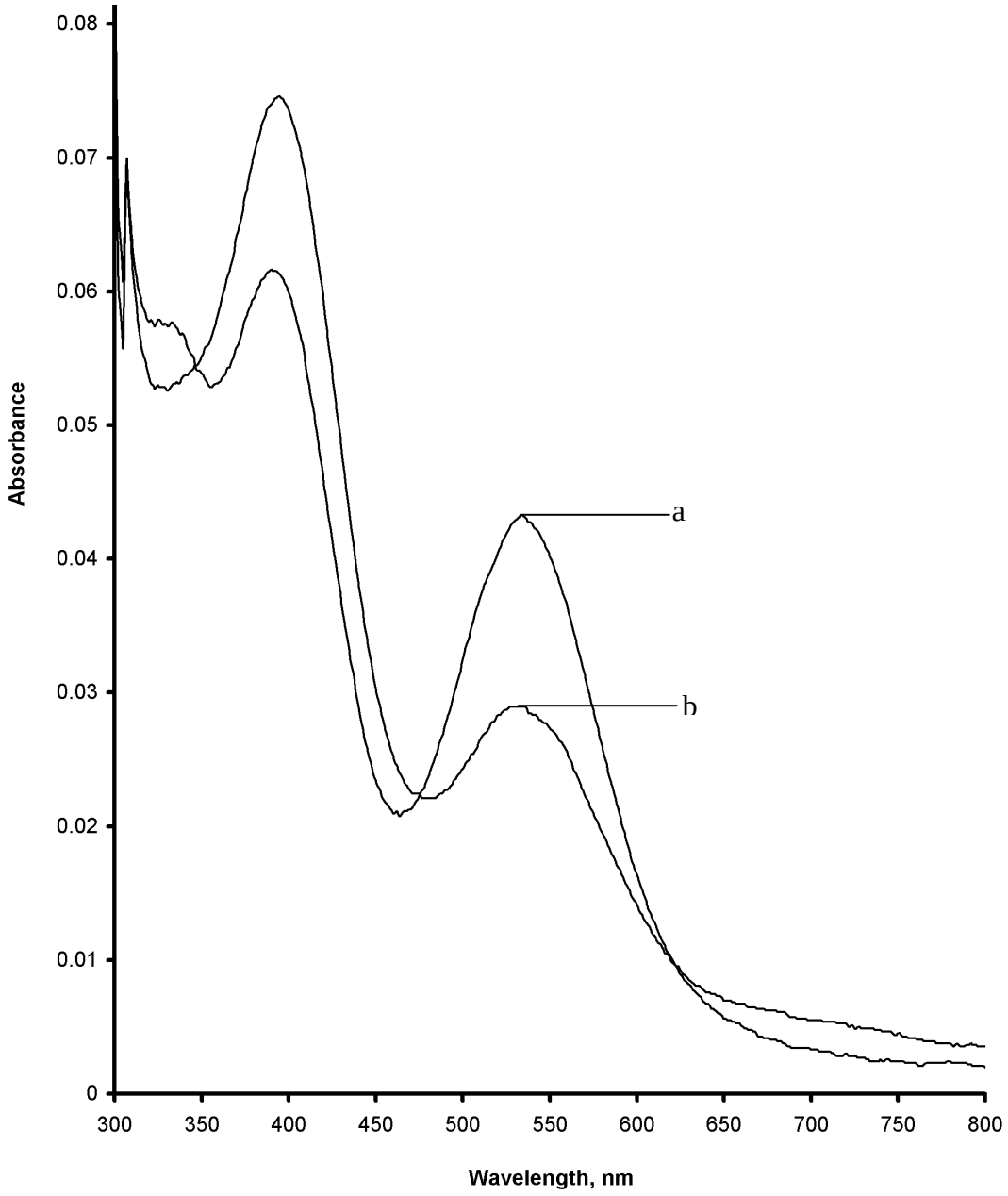

Figure 6: Spectra of the initial product of the NP-S^{2-} reaction in the presence of KCl (1M) (a) and in absence of KCl (b) at pH 11.5, 0.03 mM S^{2-} and 1 mM NP.

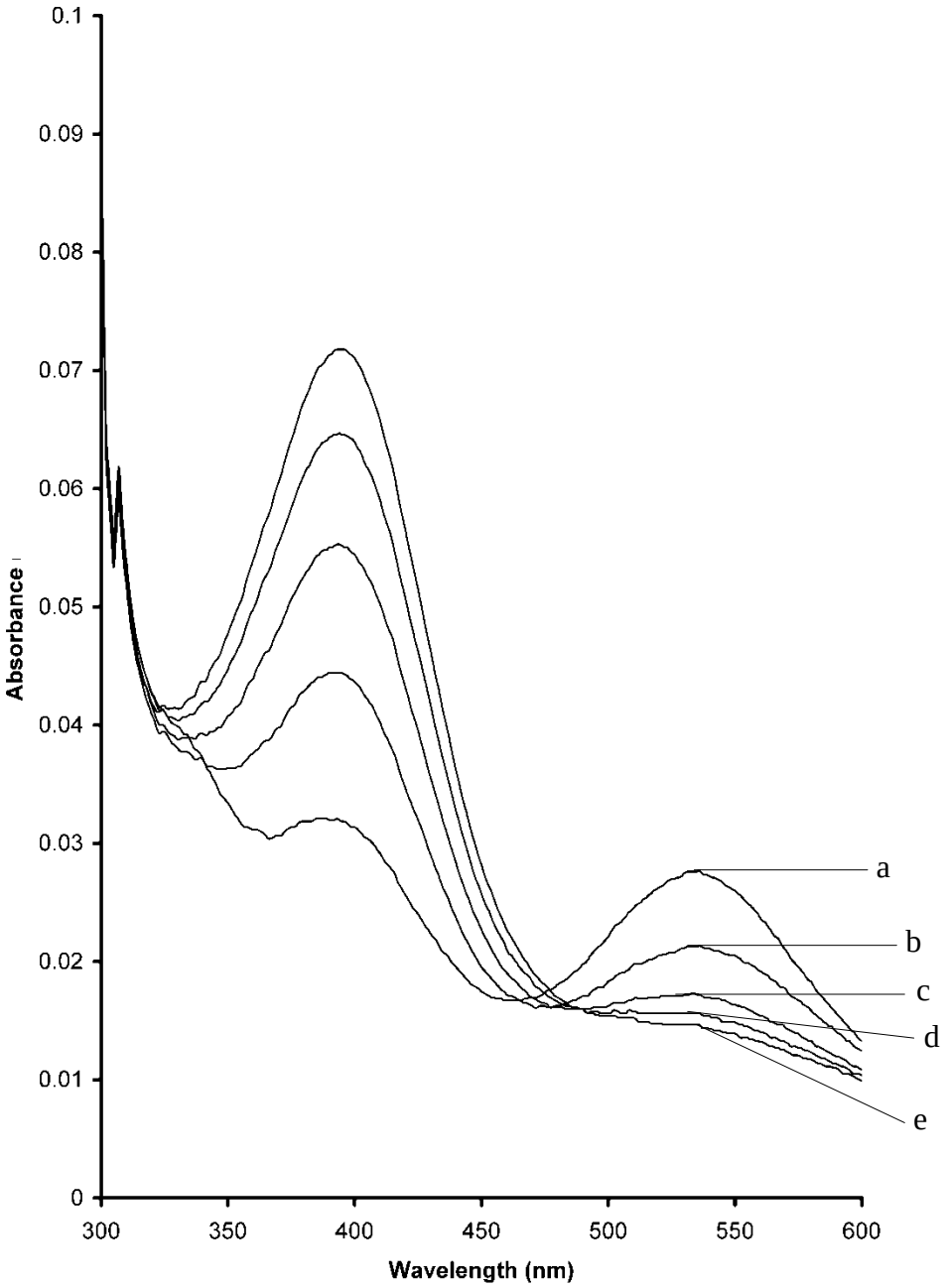

Figure 7: The time-dependent spectra of the initial product of the NP-S^{2-} reaction in the presence of KCl (1 M) in 25 seconds intervals [25 (a), 50 (b), 75 (c), 100 (d), 125 (e] at pH 11.5, 0.02 mM S^{2-} and 1 mM NP.

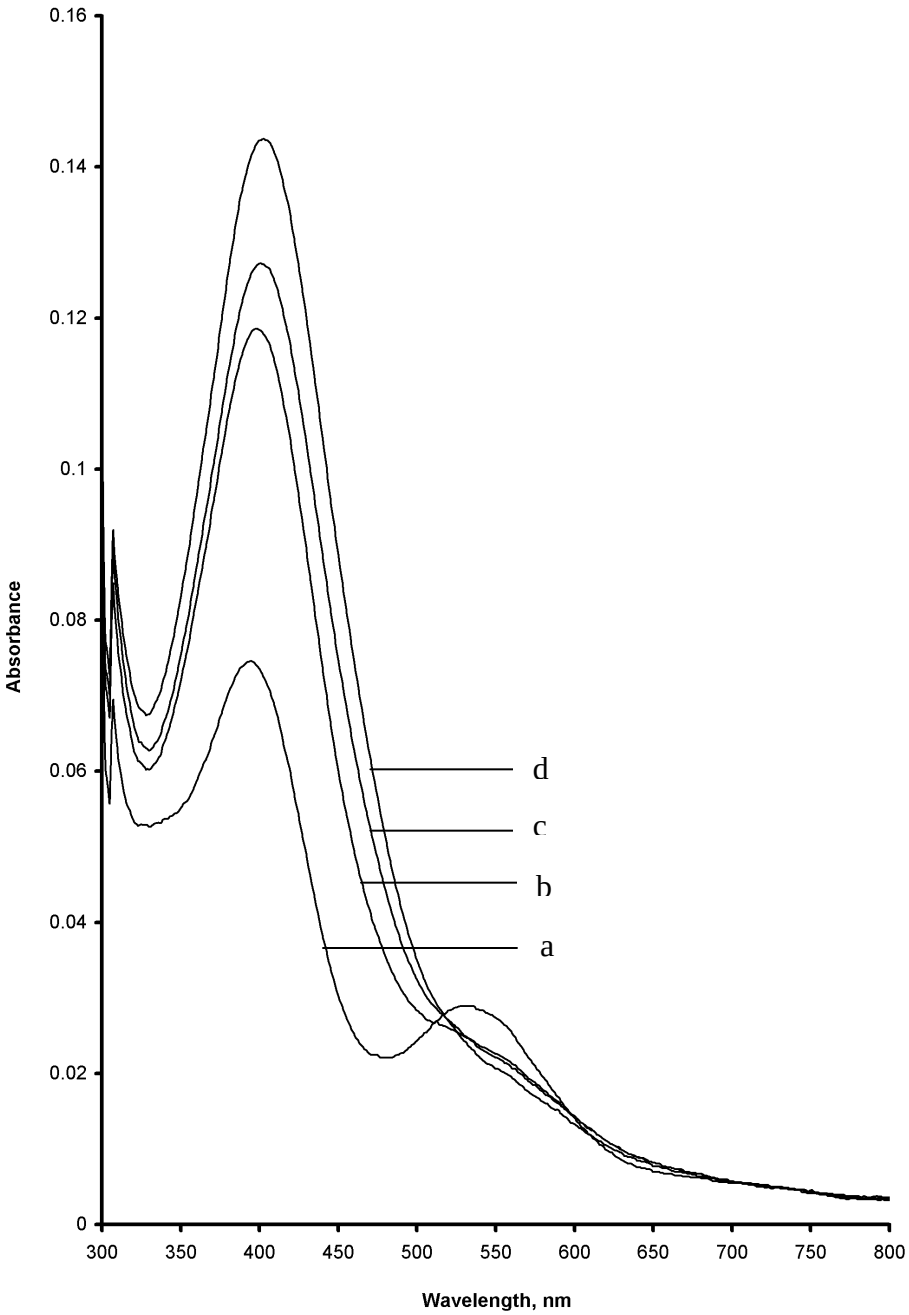

Figure 8: Time-dependent spectra of the initial product of the NP-S^{2-} reaction in the presence of KCl (1M) after periods of 1 minute (a), 4 minutes (b), 8 minutes (c) and 24 minutes (d) at pH 11.5, 0.02 mM S^{2-} and 1 mM NP.

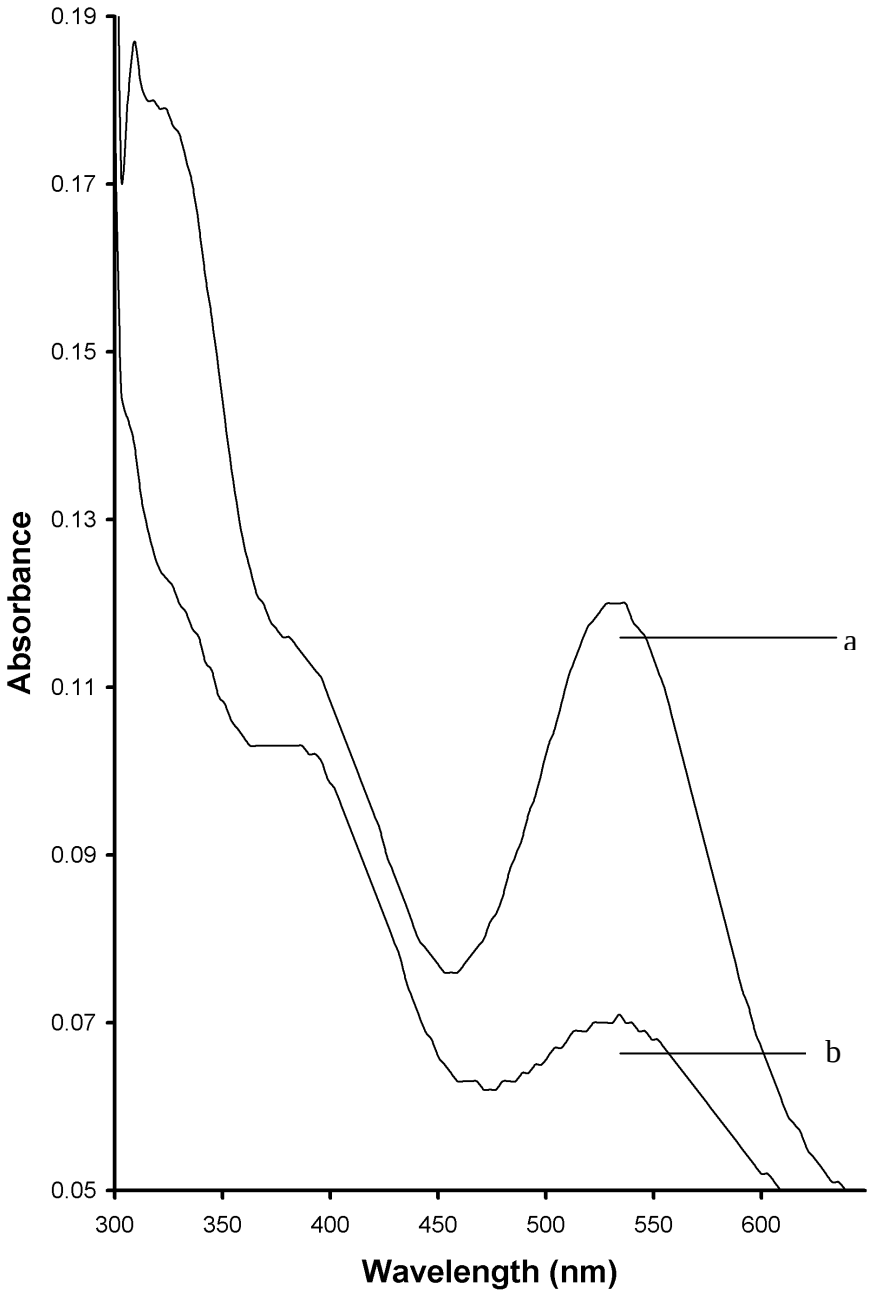

Figure 9: Visible absorption spectra of the initial product of the NP-S^{2-} reaction in the presence of KCl (1M), CN^- (0.02 M) (a) and absence of CN^- (b) at pH 11.5, 1 M KCl, 0.1 mM S^{2-} and 1 mM NP.

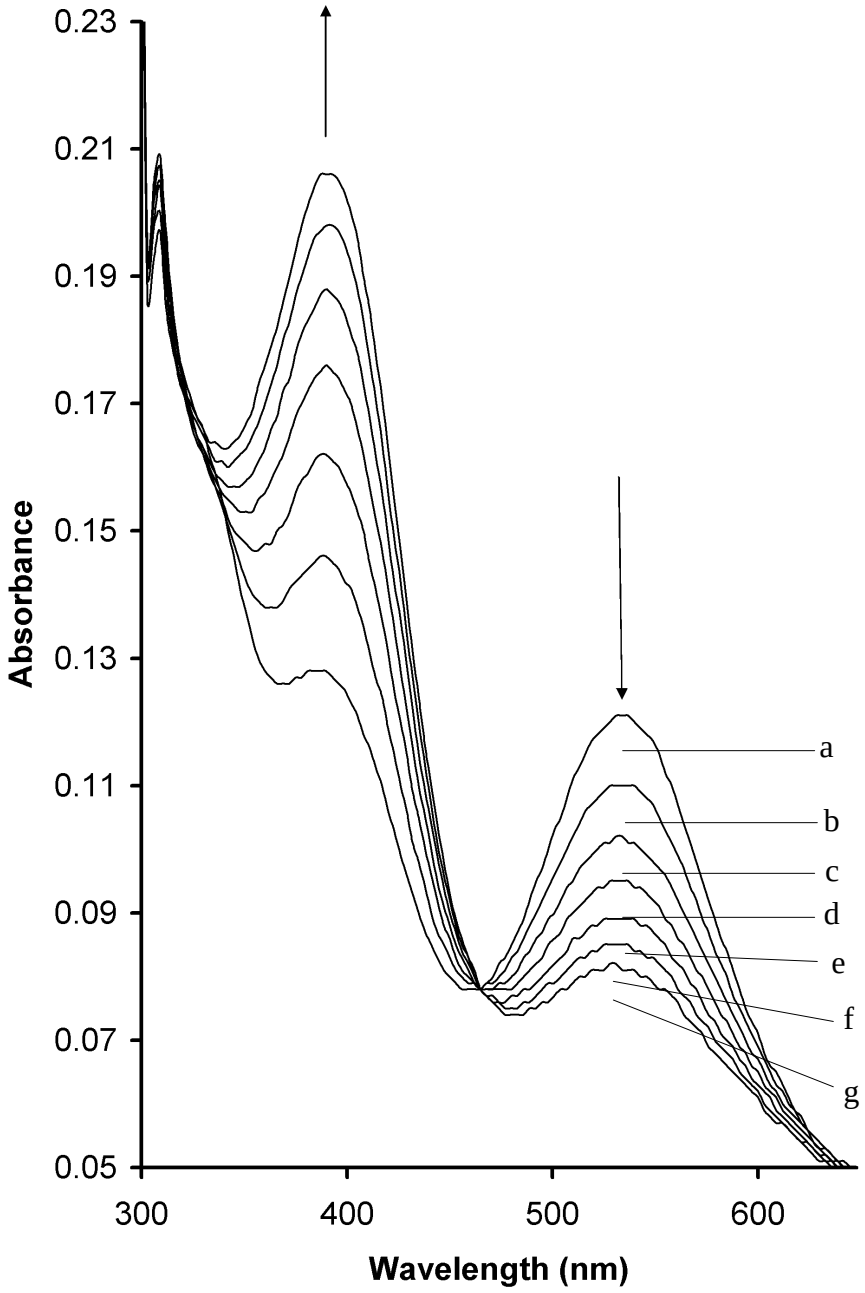

Figure 10: The time-dependent spectra of the initial product of the NP-S^{2-} reaction in the presence of KCl (1 M) and CN^- (0.02 M) in 25 seconds intervals [25 (a), 50 (b), 75 (c), 100 (d), 125 (e), 150 (f), 175 (g)] at pH 11.5, 0.1 mM S^{2-} and 1 mM NP.

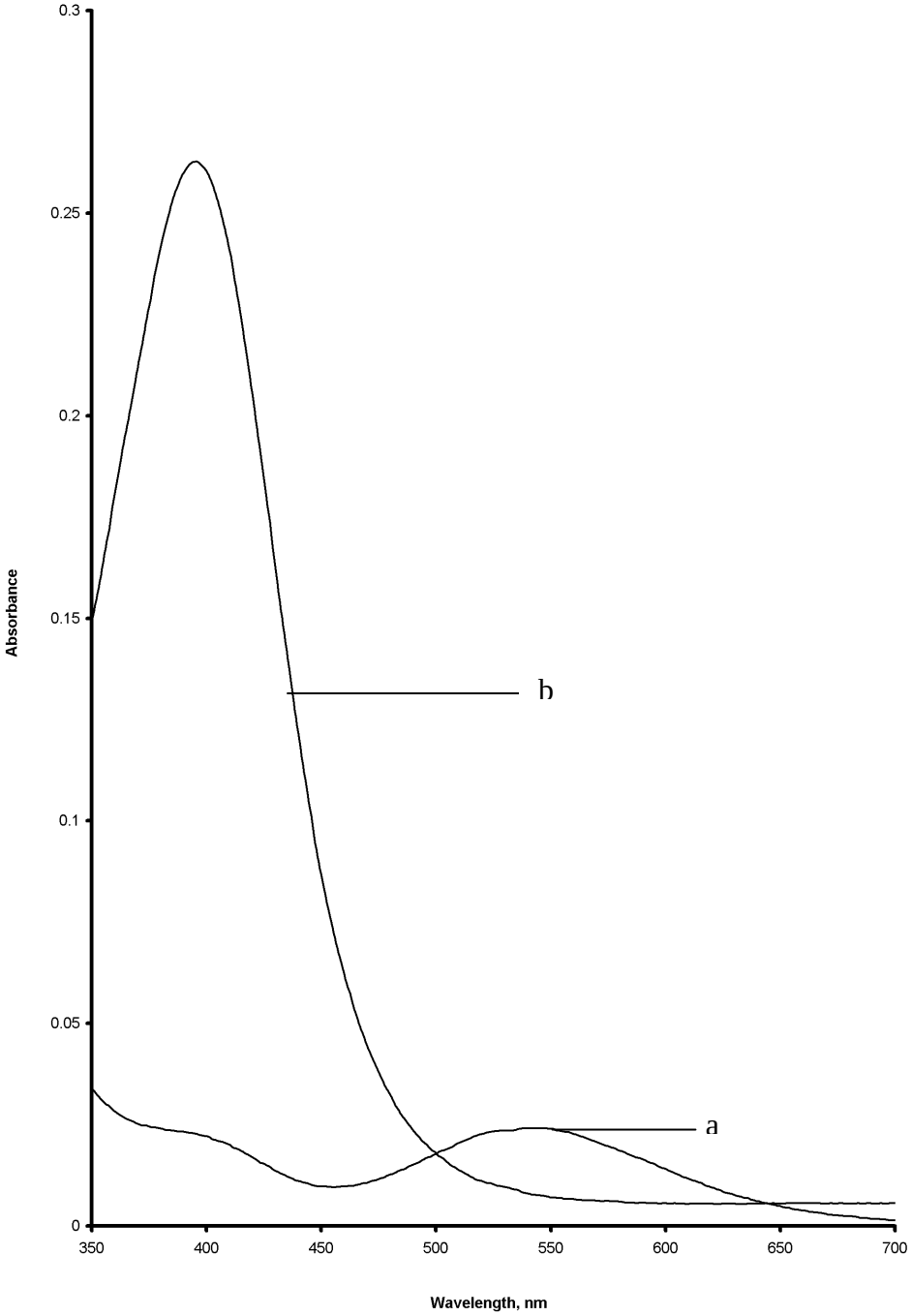

Figure 11: Spectra of the initial product of the NP-S^{2-} reaction in the presence of CN^- (0.02M) (a) and without CN^- (b) at pH 11.5, 0.02 mM S^{2-}, 1 mM NP after 30 minutes.

3.2 Kinetics of Decomposition of the Initial Product of the NP-S^{2-} Reaction

The kinetics of decomposition of the initial product in the presence of KCN and KCl in aqueous solution was studied spectrophotometrically by following the change in the absorbance of the reaction solution at 534 nm with time. It was found out that the observed rate constant k_{obs} from first-order plots increases with the concentration of the S^{2-} as illustrated in Table 2. The observed rate constant in the absence of the CN^- was difficult to follow because after a period of 1 minute a spectral characterization of this solution did not identify the characteristic λ_{max} 534 nm of the initial product, whereas in the presence of CN^- the peak of the complex at λ_{max} 534 nm was still evident even after 30 minutes as shown in Figure 11.

Table 2: Kinetic data for decomposition of the initial product of the NP-S^{2-} reaction

S^{2-} (mM)	pH	NP (mM)	KCl (M)	KCN (M)	k_{obs} x 10^3(s^{-1})
0.020	11.5	0.2	1	0.02	4.65±0.15
0.035	11.5	0.2	1	0.02	4.65±0.15
0.040	11.5	0.2	1	0.02	5.21±0.11
0.05	11.5	0.2	1	0.02	6.00±0.12
0.06	11.5	0.2	1	0.02	7.28±0.10
0.07	11.5	0.2	1	0.02	8.35±0.11

Alkali metal cations have previously been observed to affect the intensity of the coloured products in other NP reactions. This can be explained from the fact that the lone pair of electrons on the N-atom of the CN^- ligands, in transition metal cyanide complexes, are known for their marked susceptibility toward interaction with the medium [54]. For example hexacyanoferrates(II) and (III) are known to form weak ion pairs with alkali metals ions [55]. Previous studies have shown that cations play a crucial role in shifting the equilibrium between NP, thiolate and nitrosothiol complexes where small metal cations promote complex formation [56]. In these studies the authors proposed that the effect of the alkali metal cations is due to the formation of weak ion pairs which reduce the coulombic repulsion between the reacting anions thus promoting the formation of the product. The observed effect of K^+ in increasing the intensity of the initial product in this work can also be attributed to the coulombic effect K^+ introduces between NP and S^{2-} to favour formation of the initial reaction product. A proposed mechanism is summarized in equations 3.1-3.3.

$$[Fe(CN)_5NO]^{2-} + K^+ \rightleftharpoons [Fe(CN)_5NO]^{2-}.K^+ \quad (3.1)$$

$$[Fe(CN)_5NO]^{2-}.K^+ + S^{2-} \rightleftharpoons [Fe(CN)_5NO]^{2-}.K^+S^{2-} \quad (3.2)$$

$$[Fe(CN)_5NO]^{2-}.K^+S^{2-} \rightleftharpoons [Fe(CN)_5NOS]^{4-} + K^+ \quad (3.3)$$

The initial reaction product is however unstable and appears to decompose and form a yellow solution with a dorminant peak characteristic of the $[Fe(CN)_5NO_2]^{4-}$ complex.

Another factor that affects the stability of the initial reaction product is pH which was studied by Kuban et al. [5]. These authors observed an increase in the reaction rate with increase in pH accompanied with an enhanced absorbance of the products. They attributed this to increased attack of S^{2-} on the NP anion. Furthermore, the initial product was observed to be rapidly transformed into a blue product (λ_{max}574 nm), the rate of this transformation increasing with decreasing pH [5]. This work has shown that the addition of CN^- even causes a greater enhancement in absorbance at a given pH and inhibits the transformation of the initial product into the blue products. This perhaps calls for an alternative explanation of the pH effect observed by the previous workers [5]. The proposition that the red-violet initial reaction product with a λ_{max} 534 nm is $[Fe(CN)_5NOS]^{4-}$ (**I**) is maintained in this work. It has been noted that **I** can lose either CN^- or (NOS^-) [4]. The spectral changes of **I** and their dependence on CN^- concentration can be explained by the elimination of one of the CN^- ligands according to Equation (3.4) followed by its subsequent protonation shown in Equation (3.5).

$$[Fe(CN)_5NOS]^{4-} + H_2O \rightleftharpoons [Fe(CN)_4(H_2O) + CN^- \quad (3.4)$$

$$CN^- + H_2O \rightleftharpoons HCN + OH^- \quad (3.5)$$

This means there are always variable amounts of **I** and **II** present depending on the pH of the medium. Therefore, a dominant contribution of **I** should appear in the medium with increasing pH and this is consistent with the results obtained by Kuban et al. [5]. Equation (3.4) also predicts that at a given pH addition of CN^-

should cause a shift in the equilibrium of reaction to the left due to the common ion effect, resulting in a further dominance of **I** as demonstrated in Figure 9 and Figure 14.

The time-dependent spectra in respect to the decomposition of **I** display a sharp isosbestic point at 465 nm shown in Figure 9 unlike in the reported work when CN^- is absent [6]. This indicates a direct conversion of **I** to the yellow $[Fe(CN)_5(NO_2)]^{4-}$ with a λ_{max} at 398 nm . Therefore it can be proposed that the presence of the cyanide inhibits the initial formation of **II** which is probably thought to dimerize and form the blue oligomeric/ polymeric structures which are observed at low pH or in the absence of CN^- [5]. Therefore, the stabilizing effect of CN^- can be attributed to its ability to inhibit other parallel decomposition reactions of **I** and directing it to a single decomposition pathway to form $[Fe(CN)_5(NO_2)]^{4-}$. This is probably through the nucleophilic attack by the hydroxyl ions on **I** at the N atom of the (NOS).

The decomposition reaction of **I** in the presence of CN^- can be formulated in principle as composed of the elementary equilibrium reactions of Equations 3.6 and 3.7 where k_n represents the forward rate constant, and k_{-n} corresponds to the reverse rate constant.

$$[Fe(CN)_5NOS]^{4-} + OH^- \underset{k_{-1}}{\overset{k_1}{\rightleftharpoons}} [Fe(CN)_5NO_2H]^{3-} + S^{2-} \qquad (3.6)$$

$$[Fe(CN)_5NO_2H]^{3-} \underset{k_{-2}}{\overset{k_2}{\rightleftharpoons}} [Fe(CN)_5NO_2]^{4-} + H^+ \qquad (3.7)$$

The reaction rate for decomposition of **I** is given by

$$\frac{-d[Fe(CN)_5NOS]^{4-}}{dt} = k_1[Fe(CN)_5NOS]^{4-}[OH^-] - k_{-1}[Fe(CN)_5NO_2H]^{3-}[S^{2-}] \quad (3.8)$$

The reaction rate for the intermediate complex $[Fe(CN)_5NO_2H]^{3-}$ is given by

$$\frac{d\left[Fe(CN)_5NO_2H\right]^{3-}}{dt} = k_1\left[Fe(CN)_5NOS\right]^{4-}\left[OH^-\right] - k_{-1}\left[Fe(CN)_5NO_2H\right]^{3-}\left[S^{2-}\right] - k_2[[Fe(CN)_5NO_2H]^{3-} + k_{-2}[[Fe(CN)_5NO_2]^{4-}[H^+] \quad (3.9)$$

By applying steady state approximation to the intermediate complex $[Fe(CN)_5NO_2H]^{3-}$,

$$\left[Fe(CN)_5NO_2H\right]^{3-} = \frac{k_1\left[Fe(CN)_5NOS\right]^{4-}\left[OH^-\right] + k_{-2}\left[Fe(CN)_5NO_2\right]^{4-}\left[H^+\right]}{k_{-1}[S^{2-}] + k_2} \quad (3.10)$$

Substitution of $[Fe(CN)_5NO_2H]^{3-}$ into Equation 3.8 gives

$$\frac{-d\left[Fe(CN)_5NOS\right]^{4-}}{dt} = k_1\left[Fe(CN)_5NOS\right]^{4-}\left[OH^-\right] - k_{-1}\left[S^{2-}\right]\frac{k_1\left[Fe(CN)_5NOS\right]^{4-}\left[OH^-\right] + k_{-2}\left[Fe(CN)_5NO_2\right]^{4-}\left[H^+\right]}{k_{-1}[S^{2-}]+k_2}$$

which upon rearrangement becomes

$$\frac{-d\left[Fe(CN)_5NOS\right]^{4-}}{dt} = \frac{k_1k_2\left[Fe(CN)_5NOS\right]^{4-}\left[OH^-\right] - k_{-1}k_{-2}\left[S^{2-}\right]\left[Fe(CN)_5NO_2\right]^{4-}\left[H^+\right]}{k_{-1}[S^{2-}]+k_2} \quad (3.11)$$

The term $k_{-1}k_{-2}[[Fe(CN)_5NO_2]^{4-}]\ [S^{2-}]\ [H^+]$ is very small, therefore to a good approximation Equation 3.11 reduces to

$$-\frac{d\left[[Fe(CN)_5NOS]^{4-}\right]}{dt} = \left[[Fe(CN)_5NOS]^{4-}\right]\left[OH^-\right]\frac{k_1k_2}{k_{-1}[S^{2-}]+k_2} \qquad (3.12)$$

Therefore, the rate of decomposition of $[Fe(CN)_5NOS]^{4-}$ is first order in both $[Fe(CN)_5NOS]^{4-}$ and $[OH^-]$ with a second order rate constant (K) given by

$$K = \frac{k_1k_2}{k_{-1}[S^{2-}]+k_2}$$

which upon rearrangement becomes

$$\frac{k_1k_2}{K} = k_{-1}[S^{2-}]+k_2 \qquad (3.13)$$

The term $\frac{k_1k_2}{K}$ is the observed rate constant, k_{obs}, for the decomposition of $[Fe(CN)_5NOS]^{4-}$**.** Thus a plot of k_{obs} vs $[S^{2-}]$ should be linear with a positive slope which is consistent with experimental results obtained in Table 2 and Figure 12.

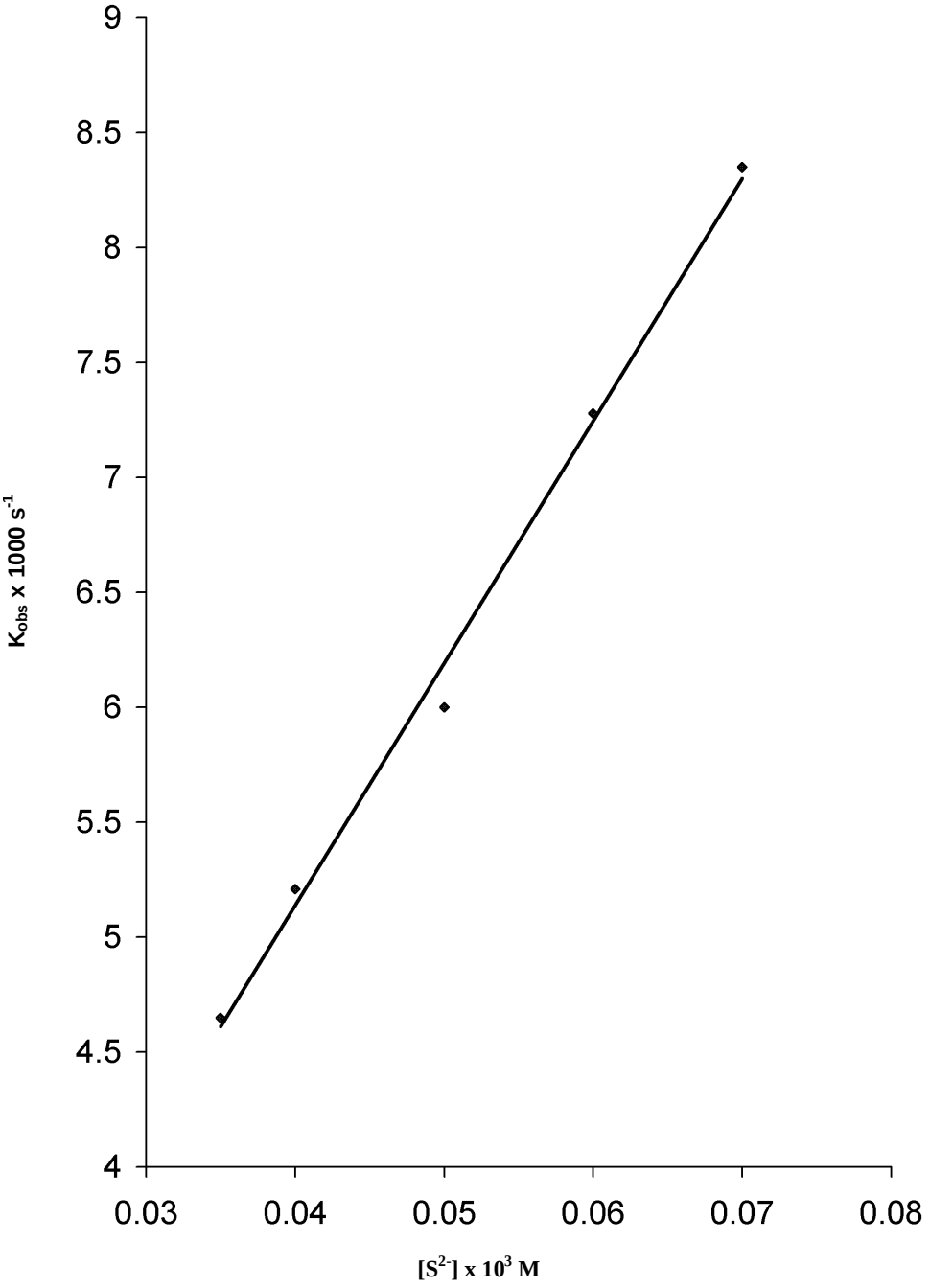

Figure 12: The linear dependence of the observed decomposition rate constant, k_{obs} of the initial product of the NP-S^{2-} reaction on the sulphide anion concentration at pH 11.5: slope = 105.4 x 10^{-3} M s^{-1}, intercept = 0.92 x 10^{-3} s^{-1}, R^2 = 0.994.

3.3 Cyanide as a Lone Stabilizer

The use of CN^- alone as a stabilizer was also investigated in this work. Upon addition of excess aqueous NP to aqueous S^{2-} containing CN^- as the stabilizer, the solution gradually become purple with a dramatic increase in the absorbance and stability of the initial product (λ_{max} 534 nm) as compared to when CN^- was absent. However, the absorbance of the solution was less than the one obtained when the reaction is carried out in the presence of alkali metal cations. Figure 13 shows a comparison of the absorption spectra obtained in the presence and absence of CN^- without alkali metal cations.

The effect of varying the CN^- concentration is shown in Figure 14 which shows a gradual increase in the absorbance of the initial reaction product (λ_{max} 534 nm) with increasing CN^- concentration. However, for higher CN^- concentrations, the decomposition rate was observed to increase as shown in Figure 15. It was further observed that a CN^- concentration in the range of 0.02-0.04 M yielded the best stabilization. Figure 18 shows how the stability of the initial reaction product absorbance was monitored for a period of thirty minutes.

The time-dependent spectra of the solution in the presence of CN^- shown in Figure 16 shows an initial increase in both $[Fe(CN)_5NOS]^{4-}$ (λ_{max} 534 nm) and ($[Fe(CN)_5NO_2]^{2-}$) (λ_{max} 398 nm). After one minute both absorbances become constant for a while followed by fall in absorbance for the $[Fe(CN)_5NO_2]^{2-}$ complex.

Figure 17 shows the spectrum of the solution after thirty minutes compared to that obtained immediately after mixing the reactants. The presence of CN^- alone further stresses clearly the stabilization of the initial product that CN^- introduces compared to when it is absent. The stabilization was optimized by carrying out the reaction in the presence of different CN^- concentrations.

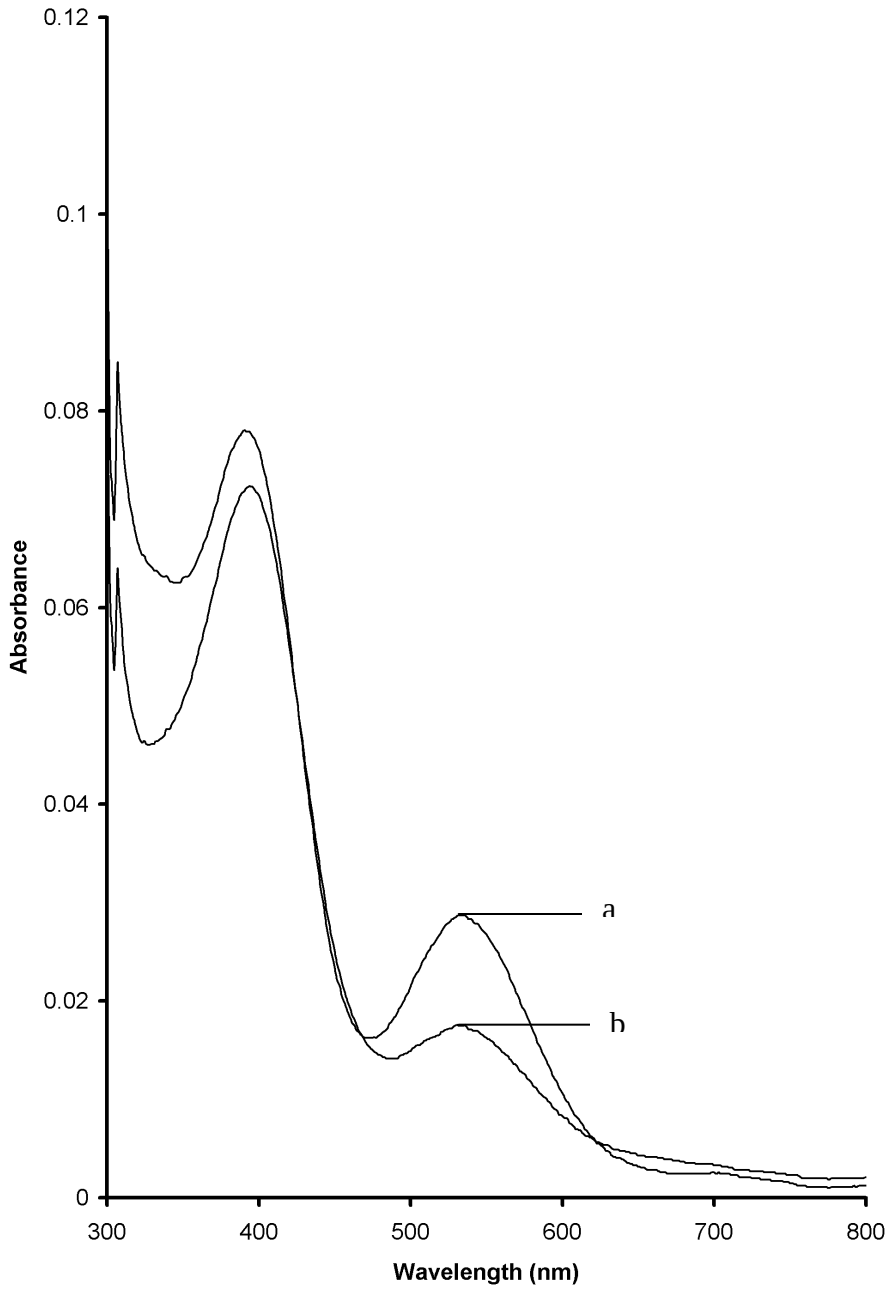

Figure 13: Visible absorption spectra of the initial product of the NP-S^{2-} reaction in the presence of CN^- (0.02 M) (a) and absence of CN^- (b) at pH 11.5, 0.1 mM S^{2-} and 1mM NP.

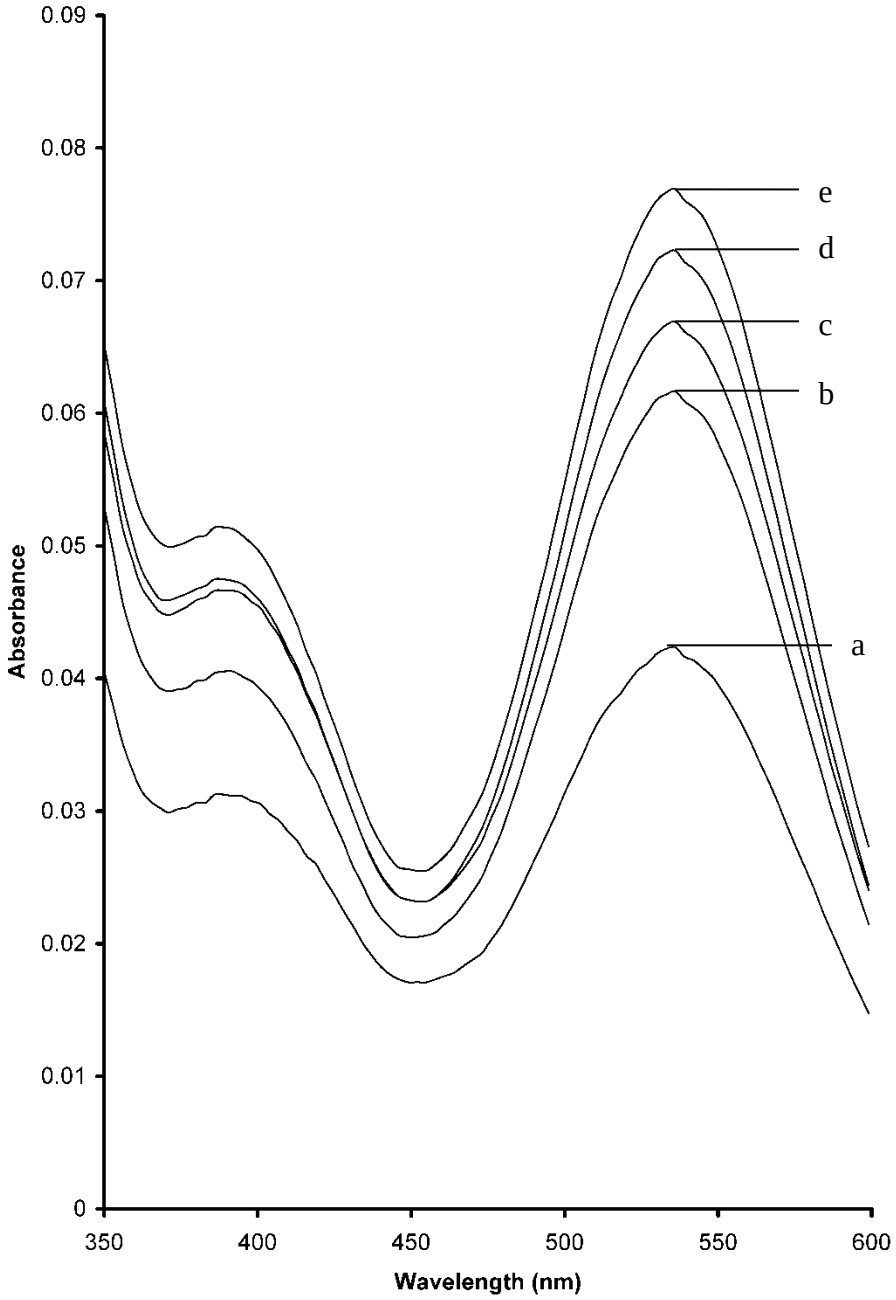

Figure 14: Visible absorption spectra of the initial product of the NP-S^{2-} reaction at cyanide concentrations of (a) 0.02 M, (b) 0.04 M, (c) 0.06 M, (d) 0.08 M, (e) 0.1 M taken after 30 seconds at pH 11.5, 0.04 mM S^{2-} and 1 mM NP.

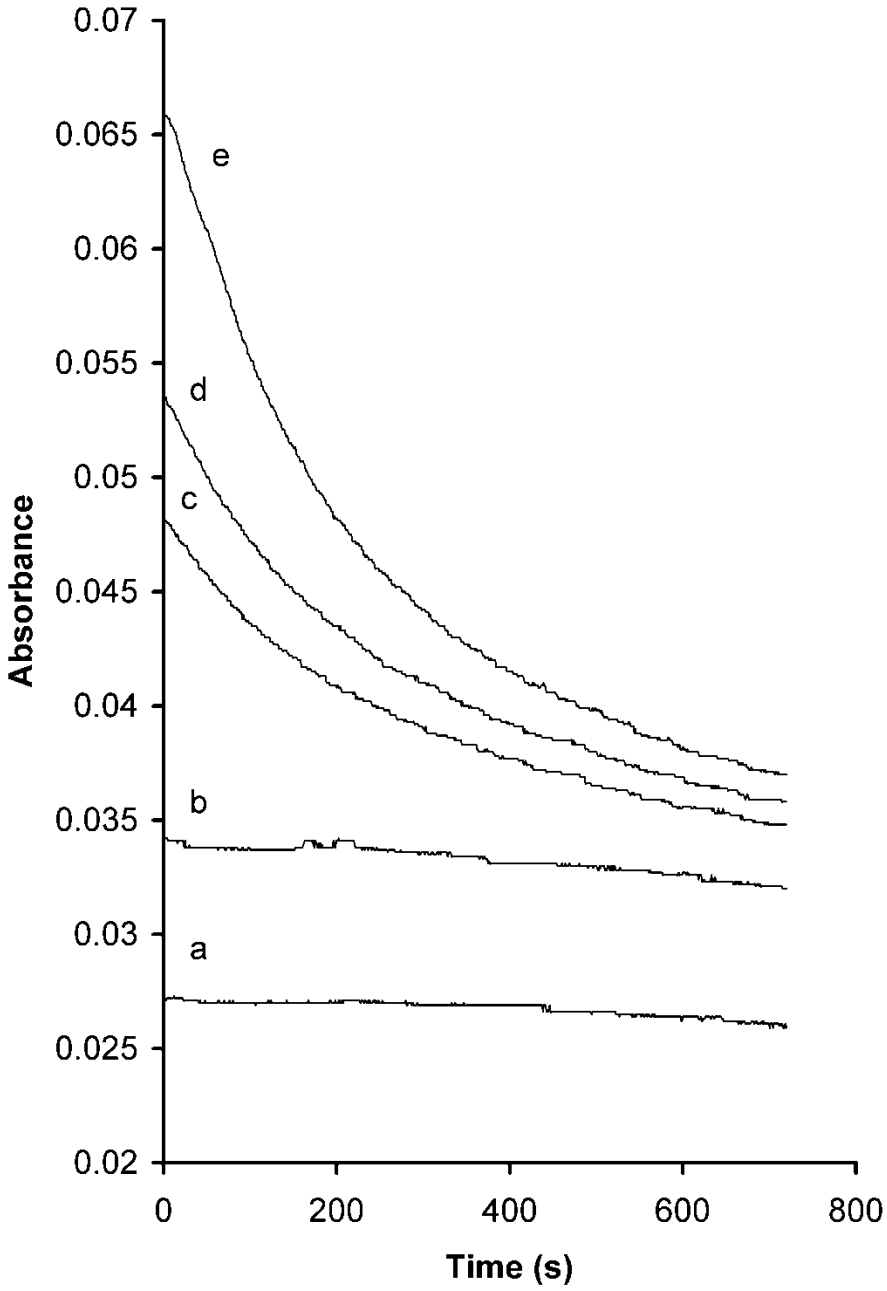

Figure 15: A time-dependent absorbance of the initial product of the NP-S^{2-} reaction at a wavelength of 534 nm in solution containing CN^- at concentrations of (a) 0.02 M, (b) 0.04 M, (c) 0.06M, (d) 0.08 M, (e) and 0.1 M at pH 11.5, 0.02 mM S^{2-}, 1 mM NP.

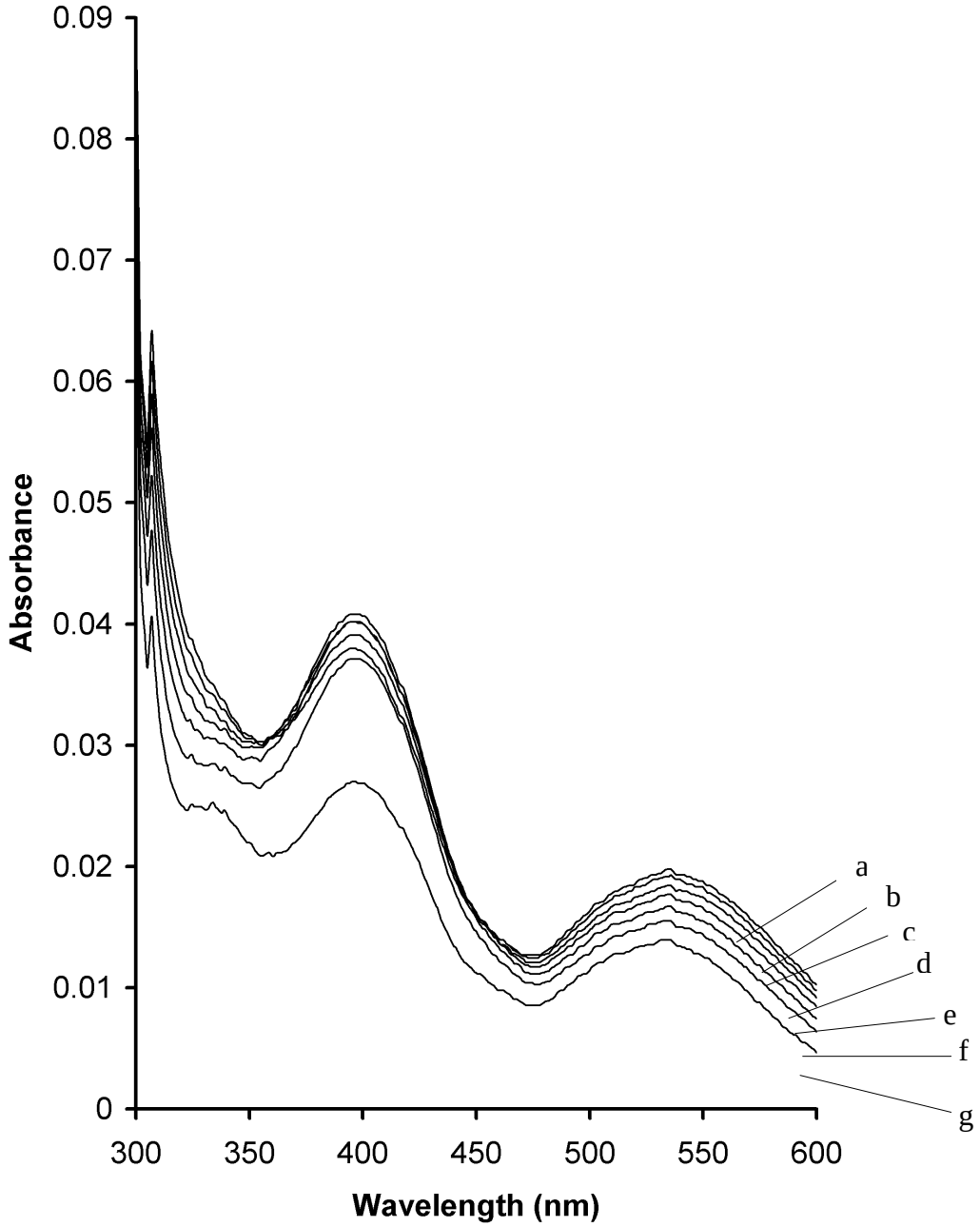

Figure 16: Time dependent spectra of the initial product of the NP-S^{2-} reaction in the presence of CN^- (0.02 M) and absence of KCl in 25 seconds intervals [25 (a), 50 (b), 75 (c), 100 (d), 125 (e), 150 (f), 175 (g)] at pH 11.5, 0.02 mM S^{2-} and 1 mM NP.

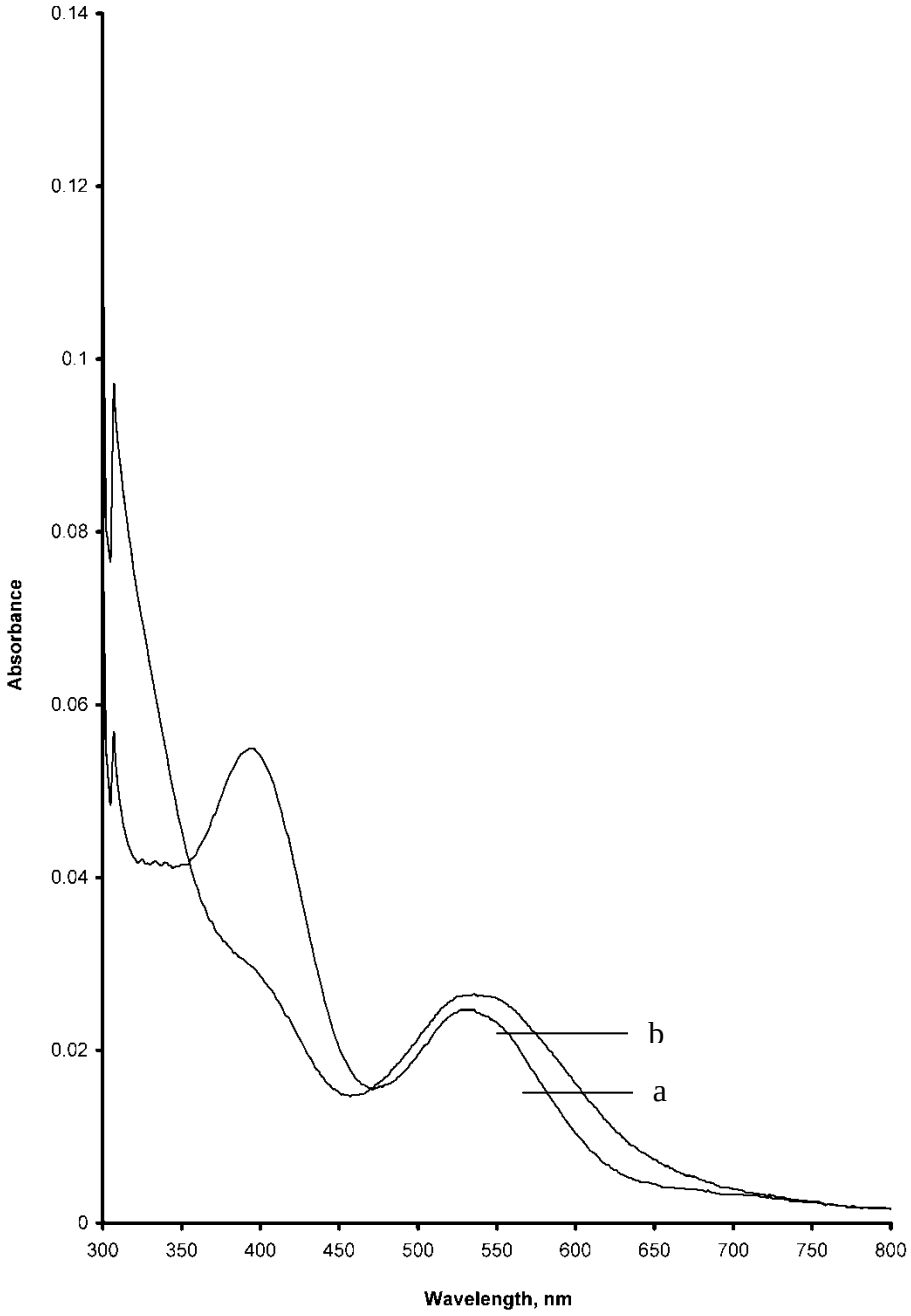

Figure 17: Spectra of the initial product of the NP-S^{2-} reaction in the absence of KCl and presence of CN^- (0.02 M) immediately after mixing (a) and after 30 minutes (b) at pH 11.5, 0.02 M S^{2-} and 1 mM NP.

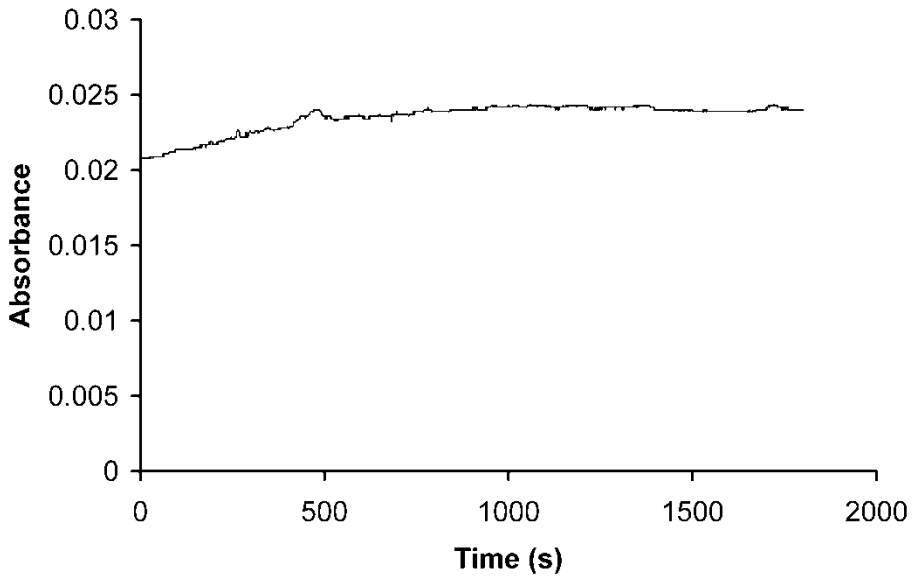

Figure 18: The variation of absorbance at 534 nm with time for the initial product of the NP-S^{2-} reaction in the presence of CN^- (0.02 M) at pH 11.5, 0.02 mM S^{2-} and 1 mM NP.

3.4 Method Development and Validation

3.4.1 Method development

For the determination of microquantities of S^{2-}, a concentration range of 0.1-5 µg mL^{-1} was considered. The optimum conditions chosen for this work were those in which CN^- was used as a lone stabilizer which was capable of stabilizing the product for a period of thirty minutes. The range of CN^- concentration used was 0.02-0.04 M, above this concentration the absorbance was further enhanced but the product was found to be very unstable and below it the sensitivity was very poor as shown in Figure 15. Figure 18 shows how the stability of the complex varies with time for a period of thirty minutes.

Basing on the results of the stabilization experiments, the spectrophotometric determination of the S^{2-} from its reaction with NP was to be carried out in aqueous alkaline media by using a phosphate buffer at pH 11.5, and CN^- concentration of 0.02 M without alkali metal cations. Absorbance readings were made after a period of 5 minutes when the absorbance was stable.

3.4.2 Method validation

3.4.2.1 Limits of detection

The LoD and LoQ for the improved method as computed from the data in Table 3 were found to be 0.2 μg mL^{-1} (Blank + 3SD) and 0.262 μg mL^{-1} (Blank + 10SD) respectively. The method has been reported to have a detection limit of 3 μg mL^{-1}. The obtained detection limits clearly show that the method has been improved dramatically and can now be applied in the detection and quantification of S^{2-} concentrations from 0.3 μg mL^{-1}.

Table 3: Determination of detection and quantification limits

Blank reading (λ_{max} 534 nm)	**Difference (x-$\bar{x}$)**	**$(x-\bar{x})^2$**
0.00122	-0.00027	7.09496×10^{-08}
0.00159	0.00010	1.07405×10^{-08}
0.00159	0.00010	1.07405×10^{-08}
0.00183	0.00034	1.18086×10^{-07}
0.00146	-2.6×10^{-05}	6.95041×10^{-10}
0.00146	-2.6×10^{-05}	6.95041×10^{-10}
0.00146	-2.6×10^{-05}	6.95041×10^{-10}
0.00146	-2.6×10^{-05}	6.95041×10^{-10}
0.0011	-0.00039	1.49277×10^{-07}
0.00098	-0.00051	2.56404×10^{-07}
0.0022	0.00071	5.09277×10^{-07}
Sum		1.12825×10^{-06}

$$SD = \sqrt{\frac{1}{n-1}\sum_{i=1}^{n}(x_i - \bar{x})^2} = \sqrt{\frac{0.00000113}{11-1}} = 0.00034$$

Standard deviation = 0.00034

Average blank value = 0.00149

Therefore LoD = 0.00149 + (3 x 0.00034) = 0.00251

LoQ = 0.00149 + (10 x 0.00034) = 0.00489

3.4.2.2 Selectivity

The effect of several cations and anions on the method was studied in detail as shown in Table 4. Different amounts of ionic species were added to the S^{2-} solution. The greatest anionic interference to this method is expected to come from SO_3^{2-} that reacts with nitroprusside in a similar manner to produce a red coloured product ($[Fe(CN)_5(NOSO_3)]^{4-}$) with λ_{max} 437 nm. In this work it was found that S^{2-} can be determined without interference from up to a SO_3^{2-} anion concentration of 1000 µg mL^{-1}.

Cationic interferences as noted in earlier work come from mainly cationic species that form sparingly insoluble sulphides like Cu^{2+} and Zn^{2+} cations. Cu^{2+} has been reported to have a significant catalytic effect on the decomposition of the reaction product. These cations seriously interfered with the reaction even at very low concentrations of up to 50 µg mL^{-1}. The use of complexones like EDTA that mask these cations is highly recommended in order to remove these interferences.

3.4.2.3 Working range and linearity

The working range was found to lie between 0.3-5 µg mL^{-1} of S^{2-} concentration, above the upper limit the decomposition of the product was relatively fast. The linearity of the calibration line obtained for S^{2-} standard solutions in the range 0.3-5 µg mL^{-1} according to its correlation coefficient was 0.9902 which implies a good linear relationship between S^{2-} concentration and absorbance. Figure 19 shows the calibration curve obtained in the concentration range 0.2-3.5 µg mL^{-1}.

The equation of the calibration line and the error in the slope and y-intercept are shown in Equation 3.15.

Table 4: The effect of a number of anions and cations on the nitroprusside method for S^{2-} in the presence of the CN^- ion, using 0.40 μg mL^{-1} S^{2-} for testing

Foreign ion added	**Interference concentration (μg mL^{-1})**	**S^{2-} recovered (μg mL^{-1})**
SO_3^{2-}	1000	0.46 ± 0.01
$S_2O_3^{2-}$	1000	0.46 ± 0.01
SCN^-	1000	0.45 ± 0.02
HPO_4^{2-}	1000	0.45 ± 0.02
Cl^-	1000	0.45 ± 0.02
Cu^{2+}	100	0
Zn^{2+}	100	0
K^+	1000	0.45 ± 0.02
Na^+	1000	0.45 ± 0.02

Table 5: Error analysis of the slope and intercept of the calibration graph

x_i	y_i	$\hat{y}_i$	$(y_i - \hat{y}_i)^2$
0.4	0.00379	0.0044	3.721×10^{-7}
0.8	0.00696	0.0070	1.60×10^{-9}
1.2	0.01099	0.0096	1.93×10^{-6}
1.6	0.01172	0.0122	2.30×10^{-7}
2.0	0.01453	0.0148	7.29×10^{-8}
2.4	0.01770	0.0174	9.00×10^{-8}
2.8	0.02026	0.0200	6.76×10^{-8}
3.2	0.02234	0.0226	6.76×10^{-8}
Sum of squared differences			2.83×10^{-6}

$$S_r = \sqrt{\frac{2.83 \times 10^{-6}}{8-2}} = 0.000687$$

$$\text{SD of the slope} = \sqrt{\frac{0.000687^2}{6.72}} = 0.000265$$

$$\text{SD of the intercept} = \sqrt{\frac{0.000687^2 \times 32.64}{8 \times 6.72}} = 0.00053$$

$$y = (0.0065 \pm 0.0003)x + (0.0018 \pm 0.0005) \quad (3.15)$$

3.4.2.4 Accuracy and precision

In this work, the accuracy of the method was validated by calculating the mean percent recovery of the spiked samples for seven replicates at three concentration

levels. A recovery of above 90% was obtained for the three concentration levels (Tables 6-8). An accuracy of more than 90% is generally considered good thus the method is deemed useful in the concentration range that was considered. The precision of the method was validated by calculating the standard deviation and RSD of the spiked samples for the seven replicates at each of the three concentration levels. For the low concentration the RSD was relatively high (15.4%), however, for higher concentrations the RSD value was low (2.4-4%). RSD values less than 20% are regarded as good therefore the method is still suitable in the concentration levels considered.

Table 6: Accuracy and precision using a 0.4 µg mL^{-1} sulphide standard solution for testing

Recovery (RV) µg mL^{-1}	**Difference (RV - 0.38)**	**Squared difference**
0.379	-0.021	0.000441
0.334	-0.066	0.004356
0.391	-0.009	0.000081
0.455	0.055	0.003025
0.384	-0.016	0.000256
0.374	-0.026	0.000676
0.349	0.051	0.002601
Sum of squared differences		0.011436

Mean value of seven replicates = 0.38 µg mL^{-1}

$$\text{Accuracy} = \frac{y}{z} \times 100\%$$

where y = mean value of seven replicates

z = spiked concentration

Therefore, for a spiked 0.4 µg mL^{-1} sulphide standard solution, the accuracy obtained according to the data in Table 6 is given by

$$\frac{0.38}{0.4} \times 100\% = 95\%$$

The SD in the determination is given by:

$$\text{SD} = \sqrt{\frac{0.011436}{7-1}} = 0.0437$$

Hence,

$$\text{RSD} = \frac{0.0437}{0.38} \times 100\% = 11.5\,\%$$

The repeatability limit is given by the formula

$$r = t_{\infty}\sqrt{2} \times \text{SD}$$

Therefore in this determination,

$$r = 1.96 \times \sqrt{2} \times 0.0437$$

= 0.12

Table 7: Accuracy and precision using a 1.5 µg mL^{-1} sulphide standard solution for testing

Recovery (RV) µg mL^{-1}	**Difference (RV - 1.6)**	**Squared difference**
1.54	-0.06	0.0036
1.62	0.02	0.0004
1.57	-0.03	0.0009
1.48	-0.12	0.0144
1.63	0.03	0.0009
1.65	0.05	0.0025
1.55	-0.05	0.0025
Sum of squared differences		0.0252

Mean value of seven replicates = 1.578 µg mL^{-1}

Therefore, for a spiked 1.5 µg mL^{-1} sulphide standard solution, the accuracy obtained according to the data in Table 7 is given by

$$\frac{1.578}{1.6} \times 100\% = 98.6\%$$

The SD in the determination is given by:

$$SD = \sqrt{\frac{0.0252}{7-1}} = 0.0648$$

Hence RSD will be:

$$\frac{0.0648}{1.578} \times 100\% = 4.1\%$$

Repeatability limit is given by the formula:

$$r = t_{\infty}\sqrt{2} \times \mathrm{SD}$$

$$r = 1.96 \times \sqrt{2} \times 0.0648$$

= 0.18

Table 8: Accuracy and precision using a 2.6 µg mL^{-1} sulphide standard solution for testing

Recovery (RV) µg mL^{-1}	**Difference (RV - 2.6)**	**Squared difference**
2.56	-0.04	0.0016
2.67	0.07	0.0049
2.65	0.05	0.0025
2.74	0.14	0.0196
2.56	-0.04	0.0016
2.63	0.03	0.0009
2.58	-0.02	0.0004
Sum of squared differences		0.0315

Mean value of seven replicates = 2.63 µg mL^{-1}

Therefore, for a spiked 2.6 µg mL^{-1} sulphide standard solution, the accuracy obtained according to the data in Table 8 is given by:

$$\frac{2.63}{2.6} \times 100\% = 101.1\%$$

The SD in the determination is given by:

$$\text{SD} = \sqrt{\frac{0.0315}{7-1}} = 0.072$$

Hence RSD will be:

$$\frac{0.072}{2.63} \times 100\% = 2.7\%$$

Repeatability limit will be:

$$r = 1.96 \times \sqrt{2} \times 0.072$$

= 0.20

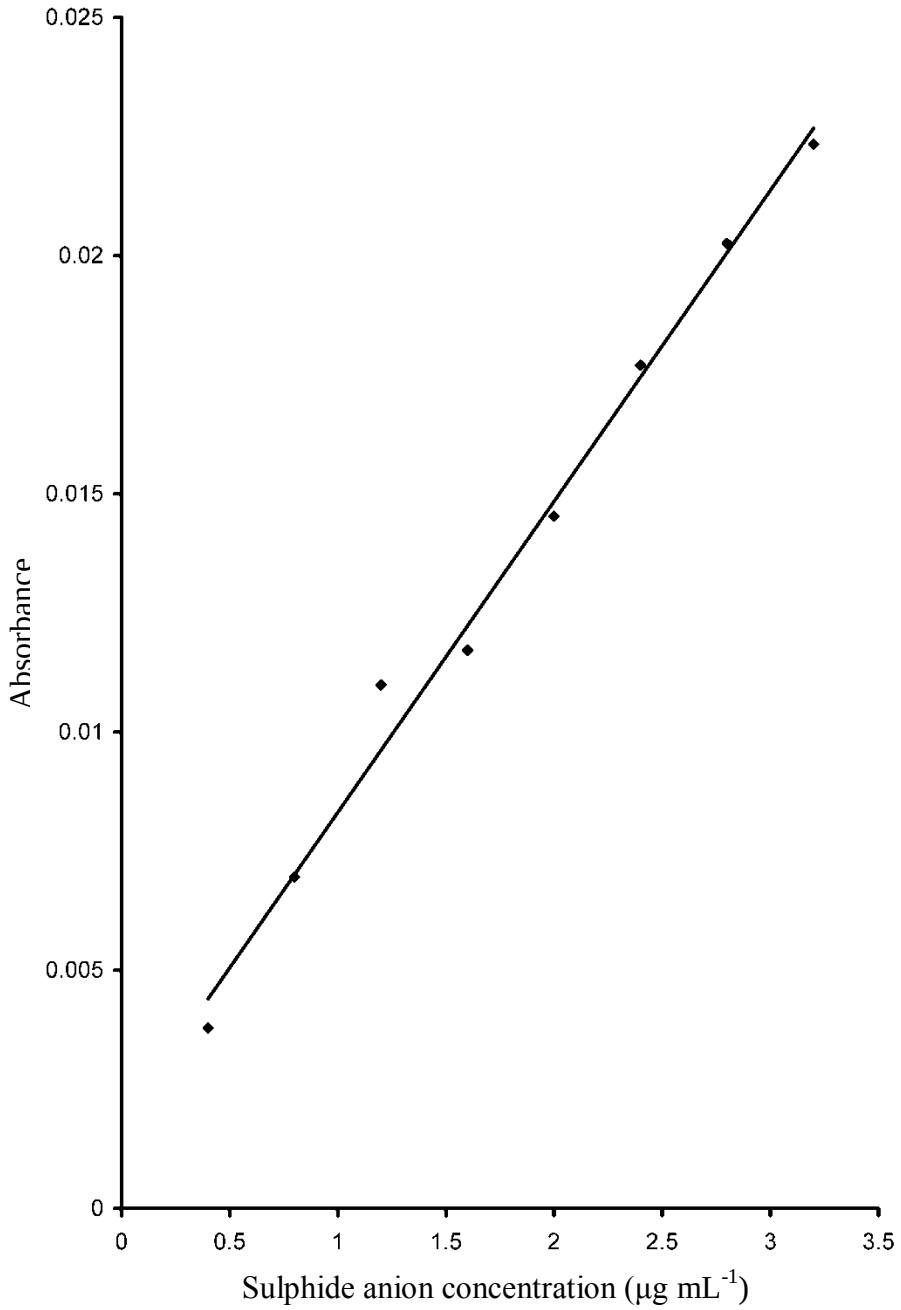

Figure 19: Calibration graph for the determination of S^{2-} using the initial product of the NP-S^{2-} reaction in the presence of CN^- (0.02 M) at pH 11.5 and 1 mM NP.

3.5 Sulphide Anion Content in Selected Environmental Systems

The method development data from section 3.4 suggests that the NP-S^{2-} reaction method in the presence of CN^- accurately assess the S^{2-} concentration dissolved in simple, well mixed solutions manufactured exclusively from H_2S dissolved in alkaline de-ionized water and also in the presence of a few interfering species. The reality in many natural environments is that S^{2-} exists not exclusively alone but in concert with many different chemical species that may interfere in its determination. The method was therefore applied to the determination of S^{2-} in a number of different environmental systems and compared to the standard iodimetric method as illustrated in Tables 9-13. The results demonstrate that S^{2-} was present in a number of environmental systems like Kitagata hot spring water where it probably arises via the hydrolysis of sulfide minerals as shown in Equation 3.16. Hot spring 2 had a lower concentration of S^{2-} than hot-spring 1 probably due to the fact that the former is still functional and is disturbed by people who bathe in it with hope that they get cured of their ailments.

$$MS(s) + H_2O(l) \longrightarrow MO(s) + H_2S(g) \qquad (3.16)$$

The results obtained from bath wastewater kept in anaerobic conditions indicate the possibility of forming H_2S in pits that collect bathroom waste water especially if bathing soap containing sulphur based detergents is used. This is due to the action of anaerobic bacteria in concert with other bacteria on organic sulphur to form H_2S.

Chicken eggs have been used as valuable nutrition sources for daily life. After the eggs have been boiled for eating, the freshness of the boiled eggs tends to deteriorate rapidly. Accordingly, boiled eggs should be eaten soon after boiling before the freshness is deteriorated. If a long time has passed before boiled eggs are eaten or if the boiled eggs are stored without taking the environmental temperature into consideration, rotting of the boiled eggs is accelerated. It is understood that eating boiled eggs in a rotted state can endanger the health of individuals. One of the key indicators of rotting in eggs is the presence of H_2S. Results obtained from boiled eggs distillate collected from a local canteen at Makerere University indicate the presence of considerable levels of H_2S in boiled chicken eggs sold for human consumption. This is due to the breakdown of sulphur based proteins to form H_2S probably due to bacterial activity.

Stagnant wastewater has the potential to generate H_2S gas especially at the bottom where anoxic conditions can develop. Results obtained from foul smelling stagnant kitchen wastewater collected from a blocked drainage man hole indicate the presence of dissolved S^{2-} in this water. This is probably due to the breakdown of sulphur based compounds to form H_2S as a consequence of anaerobic bacterial breakdown of these compounds.

The results obtained for the determination of the S^{2-} in a number of environmental samples show that the nitroprusside-cyanide method is suitable for the analysis of water samples in the environment and compares favourably with iodimetric method. The high values obtained by iodimetry could be due to the presence of

other reducing species which were not completely removed in the sample preparation procedure.

Table 9: Comparison of nitroprusside-cyanide spectrophotometric method to iodimetric method for the determination of sulphide anion in water from Kitagata hot spring 1

Sample number (n=6)	**Nitroprusside method** S^{2-}/μg mL^{-1}	**Iodimetric method** S^{2-}/μg mL^{-1}
1	2.3 ± 0.2	2.6 ± 0.3
2	2.2 ± 0.2	2.6 ± 0.3
3	2.3 ± 0.2	2.6 ± 0.3
4	1.9 ± 0.2	2.6 ± 0.3
5	2.3 ± 0.2	2.6 ± 0.3
6	2.0 ± 0.2	2.6 ± 0.3

Table 10: Comparison of nitroprusside-cyanide spectrophotometric method to iodimetric method for the determination of sulphide anion in water from Kitagata hot spring 2

Sample number	**Nitroprusside method**	**Iodimetric method**
(n=6)	**S^{2-}/µg mL^{-1}**	**S^{2-}/µg mL^{-1}**
1	1.4 ± 0.2	1.6 ± 0.3
2	1.3 ± 0.2	1.6 ± 0.3
3	1.4 ± 0.2	1.6 ± 0.3
4	1.6 ± 0.2	2.0 ± 0.3
5	1.1 ± 0.2	1.5 ± 0.3
6	1.1 ± 0.2	1.4 ± 0.3

Table 11: Comparison of nitroprusside-cyanide spectrophotometric method to iodimetric method for the determination of sulphide anion in bath wastewater

Sample number	**Nitroprusside method**	**Iodimetric method**
(n=6)	**S^{2-} /µg mL^{-1}**	**S^{2-} /µg mL^{-1}**
1	9.5 ± 0.2	11.4 ± 0.3
2	10.3 ± 0.2	11.5 ± 0.3
3	9.0 ± 0.2	11.6 ± 0.3
4	10.0 ± 0.2	11.5 ± 0.3
5	9.2 ± 0.2	11.4 ± 0.3
6	10.5 ± 0.2	11.5 ± 0.3
7	9.6 ± 0.2	11.6 ± 0.3

Table 12: Comparison of nitroprusside-cyanide spectrophotometric method to iodimetric method for the determination of S^{2-} in boiled egg distillate

Sample number	**Nitroprusside method**	**Iodimetric method**
(n=6)	**S^{2-}/µg mL^{-1}**	**S^{2-}/µg mL^{-1}**
1	25 ± 0.2	30 ± 0.3
2	20 ± 0.2	27 ± 0.3
3	22 ± 0.2	25 ± 0.3
4	31 ± 0.2	32 ± 0.3
5	23 ± 0.2	30 ± 0.3
6	19 ± 0.2	27 ± 0.3
7	22 ± 0.2	25 ± 0.3

Table 13: Comparison of nitroprusside-cyanide spectrophotometric method to iodimetric method for the determination of S^{2-} in stagnant wastewater from Mitchell Hall of residence, Makerere University

Sample number	**Nitroprusside method**	**Iodimetric method**
(n=6)	**S^{2-}/µg mL^{-1}**	**S^{2-}/µg mL^{-1}**
1	12 ± 0.2	14 ± 0.3
2	10 ± 0.2	13 ± 0.3
3	08 ± 0.2	12 ± 0.3
4	07 ± 0.2	12 ± 0.3
5	11 ± 0.2	14 ± 0.3
6	07 ± 0.2	12 ± 0.3
7	09 ± 0.2	13 ± 0.3

CHAPTER FOUR

CONCLUSIONS AND RECOMMENDATIONS

4.1 Conclusions

The first objective of this work was to introduce stabilizers known for other NP reactions into the NP-S^{2-} reaction system and study the stability of the red-violet initial product using UV/VIS spectrophotometry. The kinetics of the decomposition of the initial reaction product was also studied. The successful stabilization of the product by the CN^- has been demonstrated through a series of kinetic and spectral characterization tests which were addressed in detail in Chapter Four. Mechanisms were proposed to explain the stabilizing effect of the CN^- on the initial product of the reaction. The successful stabilization provided means, by which a manual spectrophotometric method for determination of microquantities can be developed using manual spectrophotometry.

The second objective of this work was to develop and validate a manual spectrophotometric method for the quantification of microquantities of S^{2-} based on the modified reaction conditions of the NP-S^{2-} reaction. Validation studies on the method were conducted under controlled conditions which included well mixed solutions derived solely from H_2S dissolved in alkaline solutions of de-ionized water. The detailed validation shown in Chapter Four indicated that the manual spectrophotometric method for S^{2-} using NP-S^{2-} reaction in the presence of the CN^-, was successful.

The third objective was to apply the developed and validated spectrophotometric method to the determination of microquantities of S^{2-} in selected environmental systems. Hot-springs water, bath waste water, boiled eggs and kitchen wastewater were chosen to test the applicability of the method. The results obtained by the developed method compared favorably with those obtained using iodimetry which is a standard method of S^{2-} determination.

4.2 Recommendations

During the course of the method development and validation, a number of suggestions have been identified and are recommended for future usage as noted below.

In this work it was observed that the ratio of excess NP to S^{2-} affects the stability of the initial product of the NP-S^{2-}. Too much excess NP causes instability of the product. It is therefore recommended that an excess not greater than tenfold is good enough for analysis.

The pH at which the analysis is done should be maintained at the same level for all analyses. A pH not less than 11 is recommended if satisfactory results are to be achieved.

Unless the reaction is carried out at a carefully controlled temperature and pH, it is inadvisable to attempt to work from any precalibrated standard curve; a standard S^{2-} solution should, instead, be included in each series of estimations.

Finally, it is hoped that the work of this dissertation can be used in future for the spectrophotometric determination of microquantities of the S^{2-} anion in a number of environmental systems.

REFERENCES

[1] N.N. Greenwood and A. Earnshaw, Chemistry of the Elements, 4 ed., Pergamon Press 1984.

[2] F.A. Cotton, G. Wilkinson, C.A. Murillo and M. Bochmann, Advanced Inorganic Chemistry, 6 ed., John Willey & Sons 1999.

[3] N.V. Sidgwick, The Chemical Elements and their Compounds, Vol. II, Clarendon 1950.

[4] P.A. Rock and J.H. Swinehart, Inorganic Chemistry 5 (1965) 1078.

[5] V. Kuban, P.K. Dasgupta and J.N. Marx, Analytical Chemistry 64 (1992) 36-43.

[6] V.F. Toropova and A. Rybkin, Zhurnal analiticheskoi Khimii 28 (1973) 1355.

[7] L.S. Clesceri, A.E. Greenberg and A.D. Eaton, Standard Methods for the Examination of Water and Wastewater, 20th ed., American Public Health Association, American Water Works Association, Water Environment Federation 1998.

[8] W.J. Mavura. in Regional Workshop on Nitrogen, Phosphorus and Sulphur Derivatives in the Environment, pp. 8, Hotel Africana, Kampala-Uganda 2005.

[9] N.J. Bethea and R.M. Bethea, Analytica Chimica Acta 61 (1972) 311.

[10] P. Caspieri, R. Scott and E.A. Simpson, Analytica Chimica Acta 45 (1969) 547.

[11] J.D. Lee, A new concise inorganic chemistry, 3 ed., Van Nostrand Reinhold, New York, 1977.

[12] P.C. Ford and I.M. Lorkovic, Chemical Reviews 102 (2002) 993-1017.

[13] J.H. Swinehart and P.A. Rock, Inorganic Chemistry 5 (1966) 573 - 576.

[14] J.A. Olabe, L.A. Gentil, G. Rigotti and A. Navaza, Inorganic Chemistry 23 (1984) 4297–4302.

[15] L.M. Baraldo, M.S. Bessega, G.E. Rigotti and J.A. Olabe, Inorganic Chemistry 33 (1994) 5890–5896.

[16] F. Roncaroli, M.E. Ruggiero, D.W. Franco, G.L. Estiu and J.A. Olabe, Inorganic Chemistry 41 (2002) 5760 -5769.

[17] L. Playfair, Annalen der Chemie 74 (1850) 317.

[18] W.G. Palmer, Experimental Inorganic Chemistry, Cambridge University Press 1965.

[19] P.T. Manoharan and W.C. Hamilton, Inorganic Chemistry 2 (1963) 1043-1047.

[20] M. Buchs. in Faculty of Science, Vol. Doctor of Philosophy, pp. 117, University of Fribourg Suisse 2001.

[21] J.A. Güida, O.E. Piro and P.J. Aymonino, Inorganic Chemistry 34 (1995) 4113.

[22] S. Haussühl, G. Schetter and T. Woike, Optical Communications 114 (1995) 219-222.

[23] T. Woike, W. Kirchner, G. Schetter, T. Barthel, H. Kim and S. Haussühl, Optics Communications 106 (1994) 6.

[24] M.D. Carducci, M.R. Pressprich and P. Coppens, Journal of the American Chemical Society 119 (1997) 2669-2678.

[25] H. Paulsen, V. Rusanov, R. Benda, C. Herta, V. Schunemann, C. Janiak, T. Dorn, A.I. Chumakov, H. Winkler and A.X. Trautwein, Journal of the American Chemical Society 124 (2002) 3007.

[26] A.R. Butler, A.M. Calsy-Harrison, C. Glidewell and P.E. Sørensen, Polyhedron 7 (1988) 1197-1202.
[27] N.E. Katz, M.A. Blesa, J. Olabe and P.J. Aymonino, Journal of Inorganic and Nuclear chemistry 42 (1980) 581-585.
[28] I. Maciejowska, Z. Stasicka, G. Stochel and R.v. Eldik, Journal of the chemical society Dalton Transactions (1999) 3643 - 3649.
[29] Á. Kathó, Z. Bódi, L. Dózsa and M.T. Beck, Inorganica Chimica Acta 83 (1984) 145-150.
[30] J.H. Tinker and J.D. Michenfelder, Anesthesiology 45 (1976) 340-354.
[31] D. Mukherjee, M.S. Feldman and R.H. Helfant, The journal of the American Medical Association 235 (1976) 2406.
[32] R.K. Stoelting, Pharmacology and Physiology in Anesthetic Practice 1999.
[33] V.N. Bernshtein and B.G. Belikov, Russian Chemical Reviews 30 (1961) 227-236.
[34] W. Moser, R.A. Chalmers and A.G. Fogg, Journal of Inorganic and Nuclear Chemistry 27 (1965) 831.
[35] Y. Nakagawa and F.L. Coe, Clinica Chimica Acta 289 (1999) 57-68.
[36] E.A. Guenther, K.S. Johnson and K.H. Coale, Analytical Chemistry 73 (2001) 3481.
[37] A.f.T.S.a.D.R. (ATSDR), Toxicological profile for hydrogen sulfide (Draft for Public Comment)
U.S. Department of Health and Human Services, Public Health Service, Atlanta, GA, 2004.
[38] B. Genga, L. Changb, C. Panb, Y. Qia, J. Zhaoa, Y. Panga, J. Dud and C. Tang, Biochemical and Biophysical Research Communications 318 (2004) 756-763.
[39] M. Whiteman, J.S. Armstrong, S.H. Chu, S. Jia-Ling, B.-S. Wong, N.S. Cheung, B. Halliwell and P.K. Moore, Journal of Neurochemistry 90 (2004) 765-768.
[40] M. Whiteman, N.S. Cheung, Y.-Z. Zhu, S.H. Chu, J.L. Siau, B.S. Wong, J.S. Armstrong and P.K. Moore, Biochemical and Biophysical Research Communications 326 (2005) 794-798.
[41] S.K. Yan, T. Chang, H. Wang, L. Wu, R. Wang and Q.H. Meng, Biochemical and Biophysical Research Communications 351 (2006) 485-491.
[42] Z. Qingyou, D. Junbao, Z. Weijin, Y. Hui, T. Chaoshu and Z. Chunyu, Biochemical and Biophysical Research Communications 317 (2004) 30-37.
[43] W. Zhao, J. Zhang, Y. Lu and R. Wang, The EMBO journal 20 (2001) 6008–6016.
[44] E. Blackstone, M. Morrison and M.B. Roth, Science 308 (2005) 518.
[45] D.L. Miller and M.B. Roth, PNAS 104 (2007) 20618.
[46] C. Szabo, Nature Reviews 6 (2007) 917-935.
[47] D. Forrest, Water Sewage Effluent 5 (1985) 20.
[48] M.R. Ceba and F.V. Jara, Analyst 107 (1982) 781.
[49] T.R. Crompton, Determination of Anions, Springer-Verlag Berlin Heideberg, Gwynedd, Great Britain, 1996.
[50] Eurachem, The fitness of purpose of analytical methods, 1st English ed. 1998.
[51] R.H.S. Thompson and D. Watson, Journal of clinical pathology 5 (1951) 25-29.
[52] H. Herrmann and S.G. Moses, Journal of biological Chemistry 158 (1945) 33.

[53] P.C. Joceyln, Biochemistry of the SH group, Academic Press, London, 1972.
[54] D.A. Estrin, L.M. Baraldo, L.D. Slep, B.C. Barja and J.A. Olabe, Inorganic Chemistry 35 (1996) 3897-3903.
[55] M.k. Basu and M.N. Das, Inorganic Chemistry 9 (1970) 2781-2783.
[56] O.R. Leeuwenkamp, C.H. Vermaat, C.M. Plug and A. Bult, Pharm Weekbl Sci 6 (1984) 195-202.